Dear Christine,

Many thanks for your hard work on our manuscript. The vast majority of suggestions you made were implemented. The few ones that were not followed are answered directly in the PDF below.

We hope to have satisfactorily accommodated your comments and that it can be now accepted for publication.

Thank you for considering our manuscript. We look forward hearing from you in due course.

Sincerely yours,

Frédéric Gazeau

Impact of dust addition on Mediterranean plankton communities under present and future conditions of pH and temperature: an experimental overview

Frédéric Gazeau[1], Céline Ridame[2], France Van Wambeke[3], Samir Alliouane[1], Christian Stolpe[1], Jean-Olivier Irisson[1], Sophie Marro[1], Jean-Michel Grisoni[4], Guillaume De Liège[4], Sandra Nunige[3], Kahina Djaoudi[3], Elvira Pulido-Villena[3], Julie Dinasquet[5,6], Ingrid Obernosterer[6], Philippe Catala[6], Cécile Guieu[1]

[1] Sorbonne Université, CNRS, Laboratoire d'Océanographie de Villefranche, LOV, 06230 Villefranche-sur-Mer, France

[2] CNRS-INSU/IRD/MNHN/UPMC, LOCEAN: Laboratoire d'Océanographie et du Climat: Expérimentation et Approches Numériques, UMR 7159, 75252 Paris Cedex 05, France

[3] Aix-Marseille Université, Université de Toulon, CNRS/INSU, IRD, MIO, UM 110, 13288, Marseille, France

[4] Sorbonne Université, CNRS, Institut de la Mer de Villefranche, IMEV, 06230 Villefranche-sur-Mer, France

[5] Scripps Institution of Oceanography, University of California San Diego, USA

[6] CNRS, Sorbonne Université, Laboratoire d'Océanographie Microbienne, LOMIC, F-66650 Banyuls-sur-Mer, France

Correspondence to: Frédéric Gazeau (f.gazeau@obs-vlfr.fr)

Abstract

In Low Nutrient Low Chlorophyll areas, such as the Mediterranean Sea, atmospheric fluxes represent a considerable external source of nutrients likely ~~supporting primary production~~ especially during ~~stratification~~ periods. These areas are expected to expand in the future due to lower nutrient supply from sub-surface waters caused by climate-driven enhanced stratification, ~~likely~~ further increasing the ~~role~~ of atmospheric deposition as a source of new nutrients to surface waters. ~~Yet,~~ whether plankton communities will react differently to dust deposition in a warmer and acidified environment remains an open question. The potential impact of dust deposition both in present and future ~~climate~~ conditions was investigated ~~through~~ three ~~perturbation~~ experiments in the open Mediterranean Sea. Climate reactors (300 L) were filled with surface water collected in the Tyrrhenian Sea, Ionian Sea and in the Algerian basin during a cruise conducted ~~in May/June 2017~~ in the frame of the PEACETIME project. The ~~experimental protocol~~ comprised two unmodified control tanks, two tanks enriched with a Saharan dust analog and two tanks enriched with the dust analog and maintained under warmer (+3 ºC) and acidified (-0.3 pH unit) conditions. Samples for the analysis of an extensive number of biogeochemical parameters and processes were taken over the duration of ~~the~~ experiments ~~(3-4 d). Here, we present the general setup of the experiments and the impacts of dust seeding with and without addressing the effects of environmental changes on nutrients and biological stocks.~~ Dust addition led to a rapid ~~and maximum input of nitrate whereas phosphate~~ release from the dust analog ~~was much smaller.~~ Our results showed that the impacts of Saharan dust deposition in three different basins of the open Northwestern Mediterranean Sea are at least as strong as those observed previously in coastal waters. ~~However, interestingly,~~ the effects of dust deposition on biological ~~stocks~~ were ~~highly~~ different ~~between~~ the three investigated stations and could not be attributed to differences in their degree of oligotrophy but rather to the initial metabolic state of the community. Ocean acidification and warming did not drastically modify the composition of the

47   autotrophic assemblage with all groups positively impacted by warming and acidification.

48   ~~Although autotrophic biomass was more positively impacted than heterotrophic biomass~~ under

49   future environmental conditions, a stronger impact of warming and acidification on

50   mineralization processes suggests a decreased capacity of Mediterranean surface plankton

51   communities to sequester atmospheric CO_2 following the deposition of atmospheric particles.

1. Introduction

Atmospheric deposition is well recognized as a significant source of micro- and macro-nutrients for surface waters of the global ocean (Duce et al., 1991; Jickells et al., 2005; Moore et al., 2013). The potential modulation of the biological carbon pump efficiency and the associated export of carbon by atmospheric deposition events are still poorly understood and quantified (Law et al., 2013). This is especially true for Low Nutrient Low Chlorophyll (LNLC) areas where atmospheric fluxes can play a considerable role in nutrient cycling and that represent 60% of the global ocean surface area (Longhurst et al., 1995) as well as 50% of global carbon export (Emerson et al., 1997). These regions are characterized by a low availability of macronutrients (N, P) and/or metal micronutrients (e.g. Fe) that can severely limit or co-limit phytoplankton growth during large periods of year.

The Mediterranean Sea is a typical example of these LNLC regions and exhibits surface chlorophyll a concentrations below 0.2 µg L^{-1} all year round over most of its area, except in the Ligurian Sea where relatively large blooms can be observed in late winter-early spring (e.g. Mayot et al., 2016). Recent assessments showed that the atmospheric input of nutrients in the Mediterranean Sea is of the same order of magnitude as riverine inputs (Powley et al., 2017), making the atmosphere a considerable external source of nutrients (Richon et al., 2018). Atmospheric deposition originates both from natural (mainly Saharan dust) and anthropogenic sources (e.g. Bergametti et al., 1989; Desboeufs et al., 2018). Dust deposition, mostly in the form of pulsed inputs, is mainly associated with wet deposition (Loÿe-Pilot and Martin, 1996). Ternon et al. (2010) reported an average annual dust flux over four years of 11.4 g m^{-2} yr^{-1} (average during the period 2003–2007) at the DYFAMED station in the Northwestern Mediterranean Sea. In this region, the most important events reported in the 2010 decade amounted to ~22 g m^{-2} (Bonnet and Guieu, 2006; Guieu et al., 2010b).

76   Atmospheric deposition provides new nutrients to ~~the~~ surface waters (Guieu et al., 2010b;

77   Kouvarakis et al., 2001; Markaki et al., 2003; Ridame and Guieu, 2002)~~, Fe (Bonnet and Guieu,~~

78   ~~2006) and other trace metals~~(Desboeufs et al., 2018; Guieu et al., 2010b; Theodosi et al., 2010),

79   ~~that represent~~ significant inputs likely supporting ~~the~~ primary production ~~especially~~ during the

80   stratification period (Bonnet et al., 2005; Ridame and Guieu, 2002), although no ~~clear~~ correlation

81   between dust and ocean color could be ~~evidenced from long series of satellite observation in that~~

82   ~~part of the basin~~ (Guieu and Ridame, 2020).

83   ~~Experimental approaches~~ have shown that wet dust deposition events in the Northwestern

84   Mediterranean Sea (the dominant deposition mode in that basin) ~~present a higher impact as a~~

85   source of bioavailable ~~fertilizing~~ nutrients compared to dry deposition. ~~Indeed,~~ wet deposition

86   provides both new N and P while dry deposition supplies ~~only~~ P and does not ~~allow to~~ stimulate

87   ~~the autotrophic community (except~~ diazotrophs; Ridame et al., 2013), resulting in no increase in

88   chlorophyll *a* concentrations and primary production (Guieu et al., 2014a). ~~This so-called~~

89   ~~fertilizing effect has been experimentally shown using both micro- and mesocosms where the~~

90   ~~wet deposition of Saharan dust analog strongly stimulated primary production and phytoplankton~~

91   ~~biomass (Guieu et al., 2014a; Ridame et al., 2014) while also modifying phytoplankton diversity~~

92   ~~(Giovagnetti et al., 2013; Lekunberri et al., 2010; Romero et al., 2011).~~ In addition, ~~besides~~

93   ~~phytoplankton,~~ dust deposition also modified ~~also the~~ bacterial ~~community~~ assemblage ~~and led~~ to

94   ~~even~~ stronger enhancements of production and~~/or~~ respiration rates (Pulido-Villena et al., 2014).

95   The carbon budget established from four artificial seeding experiments during the DUNE project

96   (Guieu et al., 2014a) showed that by stimulating predominantly heterotrophic bacteria,

97   atmospheric dust deposition can ~~enhance the heterotrophic biological behavior of these~~

98   ~~oligotrophic waters. This has the potential to~~ reduce ~~the fraction of~~ organic carbon ~~that can be~~

99   export~~ed~~ to deep waters during the winter mixing period (Pulido-Villena et al., 2008) and

100 ultimately limit net atmospheric CO_2 drawdown.

Another effect induced by Saharan dust ~~deposition is the export of particulate organic carbon (POC), as lithogenic particles~~ can ~~aggregate~~ and ballast ~~dissolved~~ organic matter (Bressac et al., 2014; Desboeufs et al., 2014; Louis et al., 2017a; Ternon et al., 2010). ~~This so-called~~ lithogenic ~~carbon pump~~ can represent a major part of the carbon export following a dust deposition event (up to 50% during the DUNE experiment; Bressac et al., 2014). Recently, Louis et al. (2017a) showed that Saharan dust deposition triggers the abiotic formation of transparent exopolymeric particles (TEP), leading to the formation of organic-mineral aggregates, a formation process that is highly dependent on the quality and quantity of TEP-precursors initially present in seawater.

In response to ocean warming and increased stratification, nutrient cycling in the open ocean ~~is being and~~ will continue to be perturbed in the next decades ~~resulting very likely in~~ regionally variable impacts (IPCC, 2019). Overall, LNLC areas are expected to expand in the future (Irwin and Oliver, 2009; Polovina et al., 2008) due to ~~a~~ thermal stratification related reduction of nutrients supply from sub-surface waters (Behrenfeld et al., 2006). As such, the role of atmospheric deposition ~~might increase~~ as ~~an alternative~~ source of new nutrients to surface waters. Ongoing warming and acidification ~~of the global ocean~~ (IPCC, 2019) are also evidenced in the Mediterranean Sea (e.g. Kapsenberg et al., 2017; The Mermex group, 2011). Whether or not plankton communities will respond differently to dust deposition in future conditions is still largely unknown. ~~Although dependent on resource availability,~~ it is well known that remineralisation by bacteria is subject to positive temperature control (López-Urrutia and Morán, 2007). ~~As under severe nutrient limitation,~~ warming has no effect on primary productivity (Marañón et al., 2018), it will most likely further push the balance towards ~~net heterotrophy in~~ oligotrophic areas.

~~With respect to ocean acidification,~~ an *in situ* mesocosm experiment conducted during the summer stratified period in the Northwestern Mediterranean Sea showed that the plankton

126 community was ~~rather insensitive to this perturbation~~ under strong nutrient limitation

127 (Maugendre et al., 2017, and references therein). ~~This is coherent with results from Maugendre et~~

128 ~~al. (2015), based on~~ a batch experiment, ~~showing that,~~ under nutrient-depleted conditions in late

129 winter, ocean acidification has a very limited impact on the plankton community and that small

130 species (e.g. Cyanobacteria) might benefit from warming with a potential decrease of the export

131 and energy transfer to higher trophic levels. In contrast, in more eutrophic coastal conditions,

132 Sala et al. (2016) showed that ocean acidification ~~exerted~~ a positive effect on phytoplankton,

133 especially on pico- and nano-~~phytoplankton~~. Similarly, Neale et al. (2014) showed ~~in a coastal~~

134 ~~ecosystem of the Alboran Sea~~ that ocean acidification could lead, ~~although moderately~~, to ~~high~~

135 chlorophyll levels under low light conditions with an opposite effect under high irradiance.

136   To date and to the best of our knowledge, there have been no attempts to evaluate the

137 behavior of plankton communities ~~after the deposition of~~ atmospheric ~~particles~~ in the context of

138 future ~~levels of~~ temperature and pH. ~~Yet, following the recommendation from Maugendre et al.~~

139 ~~(2017), any perturbation experiment for future climate conditions in the Mediterranean Sea~~

140 ~~should consider atmospheric deposition as a source of new nutrients and consider both~~

141 ~~temperature and pH as external forcings.~~ Such experiments were conducted in the ~~frame~~ of the

142 PEACETIME project (ProcEss studies at the Air-sEa Interface after dust deposition in the

143 MEditerranean sea; http://peacetime-project.org/) ~~during the cruise~~ on board the R/V "Pourquoi

144 Pas?" ~~in~~ May/June 2017. The project aimed at ~~extensively~~ studying and parameterizing the chain

145 of processes occurring in the Mediterranean Sea ~~after~~ atmospheric deposition ~~and to put them~~ in

146 ~~perspective of~~ on-going environmental changes (Guieu et al., 2020). During ~~that~~ cruise, three

147 perturbation experiments were conducted in climate reactors (300 L tanks) filled with surface

148 water collected in the Tyrrhenian Sea (TYR), Ionian Sea (ION) and ~~in the~~ Algerian basin (FAST;

149 Fig. 1). Six tanks were used to follow simultaneously and with a high temporal resolution, the

150 evolution of biological activity and stocks, nutrients ~~stocks~~, dissolved organic matter as well as

151 particles dynamics and export, following a dust deposition event simulated ~~at their surface~~, both

152 under present environmental conditions and ~~following~~ a realistic climate change scenario for

153 2100 (ca. +3 °C and -0.3 pH units; IPCC, 2013). In this manuscript, we will present the general

154 setup of the experiments and the evolution of nutrient and ~~biological stocks~~ (heterotrophic and

155 autotrophic prokaryotes, photosynthetic eukaryotes as well as micro- and meso-zooplankton).

156 ~~Several~~ other manuscripts, related to these experiments ~~and currently submitted to or published~~

157 in this special issue, focus on plankton metabolism (primary production, heterotrophic

158 prokaryote production) and carbon export (Gazeau et al., 2021), ~~on the~~ microbial food web

159 (Dinasquet et al., 2021), ~~on~~ nitrogen fixation (Céline Ridame, unpublished results) and on the

160 release of insoluble elements (Fe, Al, REE, Th, Pa) from dust (Roy-Barman et al., 2020).

2. Material and Methods

2.1. General setup

Six experimental tanks (300 L; Fig. 2), in which the irradiance spectrum and intensity can be finely controlled and ~~in which~~ future ocean acidification and warming conditions can be fully reproduced, were installed in a temperature-controlled container. The tanks are made of high-density polyethylene (HDPE) ~~and are trace-metal free in order to avoid contaminations,~~ with a height of 1.09 m, a diameter of 0.68 m, a surface area of 0.36 m^2 and a volume of 0.28 m^3. ~~All tanks were cleaned before the experimental work following the protocol described by Bressac and Guieu (2013). A weak turbulence was generated by a rotating PVC blade (9 rpm) in order to mimic natural conditions.~~ Each tank was equipped with a lid containing six rows of LEDs (Alpheus©). Each of these rows were composed of blue, green, cyan and white units in order to mimic the natural sun spectrum. At the conical base of each tank, a polyethylene (PE) bottle ~~collecting the exported material from above~~ was screwed onto a polyvinyl chloride (PVC) valve that remained open during the duration of the whole experiment. Photosynthetically active radiation (PAR; 400-700 nm) and temperature were continuously monitored in each tank using respectively QSL-2100 Scalar PAR Irradiance Sensors (Biospherical Instruments©) and pt1000 temperature sensors (Metrohm©) connected to a D230 datalogger (Consort©).

~~The experimental protocol~~ comprised two unmodified control tanks (C1 and C2), two tanks enriched with Saharan dust (D1 and D2) and two tanks enriched with Saharan dust and maintained under warmer (+3 ºC) and acidified (-0.3 pH unit) conditions (G1 and G2). The atmosphere above tanks C1, C2, D1 and D2 was flushed with ambient air (ca. 400 ppm, 6 L min^{-1}) and tanks G1 and G2 were flushed with air enriched with CO_2 (ca. 1000 ppm, 6 L min^{-1}) in order to prevent CO_2 degassing from the acidified tanks. CO_2 partial pressure ($p$$CO_2$) in both

184 ~~ambient air~~ and CO_2-enriched air was monitored using two gas analysers (LI-820, LICOR©).

185 The CO_2 concentration in the CO_2-enriched air was manually controlled through small injections

186 of pure CO_2 (Air Liquide©) using a mass flow controller.

187 ~~Three experiments were performed at the long-duration stations TYR, ION and FAST.~~

188 The tanks were filled by means of a ~~large~~ peristaltic pump (Verder© VF40 with EPDM hose,

189 flow of 1200 L h^{-1}) collecting seawater below the base of the boat (~~depth of ~~~5 m), used to

190 supply continuously surface seawater to a series of instruments during the entire campaign. In

191 order to homogeneously fill the tanks, the flow was divided into six HDPE pipes distributing the

192 water simultaneously into the different tanks. ~~Overall, the filling of the six tanks~~ took ~2 h

193 (including rinsing and initial sampling, ~~see thereafter). At the three stations, tanks were always~~

194 ~~filled at the end of the day before the start of the experiments: TYR (17/05/2017), ION~~

195 ~~(25/05/2017) and FAST (02/06/2017).~~ While filling the tanks, ~~this surface seawater was sampled~~

196 for the measurements of selected parameters (sampling time = t-12h before dust seeding, ~~see~~

197 Table 1). After filling the tanks, seawater was slowly warmed using 500 W heaters, controlled by

198 temperature-regulation units (COREMA©), ~~in G1 and G2 overnight~~ to reach an offset of +3 °C.

199 ^{13}C-bicarbonate was added to all tanks at 4:00 am (local time; Gazeau et al., 2021) and G1 and

200 G2 were acidified by addition of CO_2-saturated filtered (0.2 µm) seawater (~1.5 L in 300 L;

201 collected when filling the tanks at each station) ~~at 4:30 am~~ to reach a pH offset of -0.3. Sampl~~ing~~

202 for ~~most~~ parameters ~~took place prior to dust seeding~~ (sampling time = t0, ~~see~~ Table 1). Dust

203 seeding was ~~performed right after t0~~ between 7:00 and 9:00 (local time) in tanks D1, D2, G1 and

204 G2. The same dust analog ~~was used~~ and ~~the same dust~~ flux was ~~simulated~~ as ~~for~~ the DUNE 2009

205 experiments described in Desboeufs et al. (2014). ~~Briefly, the fine fraction (< 20 µm) of Saharan~~

206 ~~soils collected in southern Tunisia, which is a major source of dust deposition over the~~

207 ~~northwestern Mediterranean basin, was used in the seeding experiments. The particle size~~

208 ~~distribution showed that 99% of particles had a size smaller than 0.1 µm, and that particles were~~

209 mostly ~~made~~ of quartz (40%), calcite (30%) and clay (25%; Desboeufs et al., 2014). This

210 collected ~~dust~~ underwent an artificial chemical aging process by addition of nitric and sulfuric

211 acid (HNO_3 and H_2SO_4, respectively) to mimic cloud processes during atmospheric transport of

212 aerosol ~~with~~ anthropogenic acid gases (Guieu et al., 2010a, and references therein). To mimic a

213 realistic wet flux event of 10 g m^{-2}, 3.6 g of this analog dust were quickly diluted ~~into~~ 2 L ~~of~~

214 ultrahigh-purity water (UHP water; 18.2 MΩ cm^{-1} resistivity), and sprayed at the surface of the

215 tanks using an all-plastic garden sprayer (duration = 30 min). The N and P ~~total contents~~ in the

216 dust were $1.36 \pm 0.09\%$ ~~of~~ N and $0.055 \pm 0.003\%$ ~~of~~ P (see Desboeufs et al., 2014, for a full

217 description of dust chemical composition). The ~~experimental protocol included the analysis of an~~

218 ~~extensive number of~~ biogeochemical parameters and processes, ~~not all shown and discussed in~~

219 ~~this paper, and~~ are listed in Table 1. The experiment at stations TYR and ION ~~lasted 72 h (3~~

220 ~~days) whereas the last experiment~~ at station FAST ~~was extended to four days. This relatively~~

221 ~~short duration of the experiments was~~ constrained by the time available between stations ~~and the~~

222 ~~time needed to properly clean the tanks between the experiments, following the protocol~~

223 ~~described by Bressac and Guieu (2013). As a larger time window was possible at the end of the~~

224 ~~cruise, the experiment at FAST was extended to four days.~~ Seawater sampling was conducted 1

225 h (t1h), 6 h (t6h), 12 h (t12h), 24 h (t24h), 48 h (t48h) and 72 h (t72h) (+ 96 h = t96h for station

226 FAST) ~~after dust addition.~~ Acid-washed silicone tubes were used for transferring the water

227 collected from the tanks to the different vials or containers. ~~For some parameters (e.g. micro- and~~

228 ~~macro-nutrients), sampled seawater was directly filtered at the exit of the sampling tubes~~

229 ~~connected to each tank on sterile membrane filter capsules (gravity filtration with Sartobran©~~

230 ~~300; 0.2 μm).~~

2.2. Analytical methods

2.2.1. Carbonate chemistry

Seawater samples for pH measurements were stored in 300 mL glass bottles with a glass stopper, pending analysis on board (within 2 h). Samples were transferred to 30 mL quartz cells and absorbances at 434, 578 and 730 nm were measured at 25 °C on an Cary60 UV-Spectrophotometer (Agilent©) before and after addition of 50 µL of purified meta-cresol purple provided by Robert H. Byrne (University of South Florida, USA) following the method described by Dickson et al. (2007). pH on the total scale (pH_T) was computed using the formula and constants of Liu et al. (2011). The accuracy of pH measurements was estimated ~~to 0.007 pH units~~, using a TRIS buffer solution (salinity 35, provided by Andrew Dickson, Scripps university, USA).

Seawater samples for total alkalinity (A_T~~; 500 mL~~) measurements were filtered on GF/F membranes and analyzed onboard within one day. A_T was determined potentiometrically using a Metrohm© titrator (Titrando 888) and a glass electrode (Metrohm©, ecotrode plus) calibrated using first NBS buffers (pH 4.0 and pH 7.0, to check that the slope was Nernstian) and then using a TRIS buffer solution (salinity 35, provided by Andrew Dickson, Scripps university, USA). Triplicate titrations were performed on 50 mL sub-samples at 25 ºC and A_T was calculated as described by Dickson et al. (2007). Titrations of standard seawater provided by Andrew Dickson (Scripps university, USA; batch 151) yielded A_T values within 5 µmol kg^{-1} of the nominal value (standard deviation = 1.5 µmol kg^{-1}; n = 40).

All parameters of the carbonate chemistry were determined from pH_T, A_T, temperature, salinity, as well as phosphate and silicate concentrations using the R package seacarb. Propagation of errors on computed parameters was performed using the new function "error" of

254 this package, ~~considering~~ errors associated with the estimation of A_T, pH$_T$ as well as errors ~~on~~

255 dissociation constants (Orr et al., 2018).

2.2.2. Nutrients

257 Seawater samples for dissolved nutrients were ~~filtered directly at the exit of~~ the sampling

258 tubes ~~connected to~~ each tank (Sartobran© 300; 0.2 μm), ~~collected in polyethylene bottles~~ and

259 ~~immediately~~ analyzed on board. Nitrate + nitrite (NO_x) and silicate ($Si(OH)_4$) measurements

260 were conducted using a segmented flow analyzer (AAIII HR Seal Analytical©) according to

261 Aminot and Kérouel (2007) with a limit ~~of quantification~~ of 0.05 μmol L^{-1} for NO_x and 0.08

262 μmol L^{-1} for $Si(OH)_4$. In addition, ~~for t-12h samples, the analysis of~~ NO_x was also ~~performed~~ by

263 ~~a spectrometric method in the visible~~ at 540 nm, with a 1 m Liquid Waveguide Capillary Cell

264 (LWCC). ~~The limit of detection was~~ ~10 nmol L^{-1} and ~~the~~ reproducibility ~~was~~ ~6%. ~~Also from~~

265 ~~samples taken at t-12h, the measurement of~~ ammonium concentrations ~~was performed~~ on board

266 using a Fluorimeter TD-700 (Turner Designs©) according to Holmes et al. (1999). This

267 ~~fluorimetric~~ method is based on the reaction of ammonia with orthophtaldialdehyde and sulfite

268 and has a limit ~~of quantification~~ of 0.01 μmol L^{-1}. Dissolved inorganic phosphorus (DIP)

269 concentrations were quantified using the Liquid Waveguide Capillary Cell (LWCC) method

270 according to Pulido-Villena et al. (2010). The LWCC was 2.5 m long and the limit ~~of detection~~

271 was 1 nmol L^{-1}.

2.2.3. Pigments

273 ~~A volume of 2.5 L of sampled seawater was~~ filtered onto GF/F filters, immediately

274 frozen in liquid nitrogen and stored at -80 ºC pending analysis at the SAPIGH analytical platform

275 at the Institut de la Mer de Villefranche (IMEV, France). Filters were ~~extracted~~ at -20 ºC in 3 mL

276 methanol (100%) containing an internal standard (vitamin E acetate, Sigma©), ~~disrupted by~~

277 ~~sonication~~ and clarified one hour later by vacuum filtration through GF/F filters. The extracts

278 were rapidly analyzed (within 24 h) on a complete Agilent© Technologies 1200 series HPLC

279 system. The pigments were separated and quantified as described in Ras et al. (2008).

2.2.4. Flow cytometry

281 For ~~the enumeration of autotrophic prokaryotic and eukaryotic cells, heterotrophic~~

282 ~~prokaryotes and heterotrophic nanoflagellates (HNF) by~~ flow cytometry, ~~sub~~samples (4.5 mL)

283 were fixed with glutaraldehyde grade I ~~25%~~ (1% final concentration), and incubated for 30 min

284 at 4 °C, ~~then~~ quick-frozen in liquid nitrogen and stored at -80 °C until analysis. Samples were

285 thawed at room temperature. Counts were performed on a FACSCanto II flow cytometer (Becton

286 Dickinson©) equipped with 3 air-cooled lasers: blue (argon 488 nm), red (633 nm) and violet

287 (407 nm). ~~The separation of different autotrophic populations was based on their scattering and~~

288 ~~fluorescence signals according to~~ Marie et al. (2010)~~,~~ *Synechococcus* spp. was discriminated by

289 its strong orange fluorescence (585 ± 21 nm), and pico- and nano-eukaryotes were discriminated

290 by their scatter signals of red fluorescence (> 670 nm). For the enumeration of heterotrophic

291 prokaryotes, cells were stained with SYBR Green I (Invitrogen – Molecular Probes) at 0.025%

292 (vol / vol) final concentration for 15 min at room temperature in the dark. Stained prokaryotic

293 cells were discriminated and enumerated according to their right-angle light scatter (SSC) and

294 green fluorescence at 530/30 nm. ~~In a plot of green versus red fluorescence,~~ heterotrophic

295 prokaryotes were distinguished from autotrophic prokaryotes. For the enumeration of HNF,

296 ~~staining was performed with SYBR Green I (Invitrogen – Molecular Probes) at~~ 0.05% (v/v) final

297 concentration for 15-30 min at room temperature in the dark (Christaki et al., 2011). ~~Cells were~~

298 ~~discriminated and enumerated according to their SSC and green fluorescence at 530/30 nm.~~

299 Fluorescent beads (1.002 µm; Polysciences Europe©) were ~~systematically~~ added to ~~each~~

300 ~~analyzed~~ sample as internal standard. ~~The cell abundance was~~ determined ~~from the~~ flow rate,

301 ~~which was calculated~~ with TruCount beads (BD biosciences©). Biomass~~es~~ of each group were

302 estimated based on conversion equations and/or factors found in the literature (see section 2.3.2).

2.2.5. Micro-phytoplankton and -heterotrophs

304 At t-12h ~~(i.e. seawater sampled during the filling of the tanks), a volume of~~ 500 mL was

305 ~~sampled~~ in glass vials and immediately preserved ~~in a~~ 5% acidic Lugol's solution ~~pending~~

306 ~~analysis.~~ At the Laboratoire d'Océanographie de Villefranche (LOV, France), 100 mL aliquots

307 were transferred to sedimentation chambers (Utermohl) and counted under an inverted

308 microscope at 200 to 400 magnification~~s~~.

2.2.6. Mesozooplankton

310 At the end of each experiment ~~(t+72h for TYR and ION and t+96 h for FAST, after~~

311 ~~artificial dust seeding)~~, the ~~sediment traps~~ were removed, ~~closed and stored~~ with formaldehyde

312 4% (see Gazeau et al., 2021). ~~The~~ valve at the base of ~~the~~ tanks was ~~then reopened~~ ~~to let~~ the

313 remaining water inside the tanks (~~TYR~~ 165-180 L; ~~ION =~~ 172.5 L and ~~FAST =~~ 150 L) ~~pass~~

314 through a ~~large~~ PVC sieve (100 µm). The organisms retained ~~on that mesh~~ were gently removed

315 ~~from the sieve~~ using a washing bottle filled with filtered seawater (0.2 µm), and transferred

316 directly in~~side~~ a 250 mL bottle. ~~The bottle was filled with the sample (1/3 of the volume), and~~

317 ~~was completed with formaldehyde 4%. The zooplankton digital images were obtained~~ using a

318 ZooSCAN (Hydroptic©; Gorsky et al., 2010) at the PIQv-platform of EMBRC-France. ~~The~~

319 ~~identification of species was performed by~~ automatic classification with a reference dataset in

320 EcoTaxa (https://ecotaxa.obs-vlfr.fr/, last access: 17/04/2020) and ~~then all~~ validat~~ed and~~

321 ~~corrected manually~~.

2.3. Data analyses

2.3.1. Nutrient inputs from dust

The maximum percentage of dust-born dissolved N and P was calculated considering that these evapo-condensated dust contain $1.36 \pm 0.09\%$ of N and $0.055 \pm 0.003\%$ of P (Desboeufs et al., 2014). Based on maximal concentrations observed in the D and G tanks after seeding (two discrete sampling within 6 h following dust seeding, t1h and t6h), one can estimate the maximal % of dissolution of dust in seawater during the three experiments:

$$\%_{dissolution} = \frac{CONC_{max} - CONC_{init}}{CONC_{dust}} \cdot 100 \qquad (1)$$

where $CONC_{init}$ is the concentration of the corresponding nutrient in each tank before seeding (t0), $CONC_{max}$ corresponds to the concentration of the corresponding nutrient in each tank when nutrient concentration was at a maximum over the first 6 h after seeding as observed based on our discrete sampling procedure, and $CONC_{dust}$ is the maximum addition, corresponding to a 100% dissolution of its total concentration in the dust analog (as estimated based on dust chemical composition; Desboeufs et al., 2014; see above).

2.3.2. Autotrophic and heterotrophic biomass

As micro-phytoplankton counting was not performed throughout the experiment, as a first approximation, autotrophic biomass was calculated as the sum of carbon contained in *Synechococcus*, pico-eukaryotes and nano-eukaryotes (abundances based on flow cytometry) and is therefore restricted to the fraction < 20 μm. For *Synechococcus*, conversion to carbon units was done considering 250 fg C cell[-1] (Kana and Glibert, 1987), while the equation proposed by Verity et al. (1992; $0.433 \, BV^{0.863}$ where BV refers to the biovolume) was used for pico- and nano-eukaryotes assuming a spherical shape and a diameter of 2 and 6 μm for the two groups,

344   respectively. ~~Percentages of these different groups were calculated in order to estimate the~~

345   ~~composition of the communities at the start and its evolution during the experiments.~~

346   ~~Furthermore,~~ heterotrophic biomass was computed as the sum of heterotrophic prokaryotes

347   ~~biomass~~ and heterotrophic nanoflagellates biomass. ~~For heterotrophic prokaryotes, conversion to~~

348   carbon ~~units were done considering~~ 20 fg C cell^{-1} (Lee and Fuhrman, 1987) and ~~for heterotrophic~~

349   ~~nanoflagellates assuming~~ 220 fg C μm^{-3} (Børsheim and Bratbak, 1987), a spherical shape ~~and a~~

350   ~~diameter~~ of 3 μm. The ratio of autotrophic and heterotrophic biomass during the experiments was

351   used to evaluate the trophic status of the investigated communities and its evolution. Finally, a

352   proxy for micro-phytoplankton biomass (B_{micro}) was estimated following Vidussi et al. (2001), as

353   the sum of Fucoxanthin and Peridinin.

3. Results

3.1. Initial conditions

Initial conditions at the three sampling stations while filling the tanks (t-12h before seeding) are shown in Table 2. pH_T total alkalinity concentrations (8.03, 8.04 and 8.07; 2443, 2529 and 2627 $\mu mol\ kg^{-1}$ at FAST, TYR and ION, respectively), NO_x concentrations were maximal at station FAST with a NO_x:DIP molar ratio of ~ 4.6. Very low NO_x concentrations were observed at stations TYR and ION (14 and 18 nmol L^{-1}, respectively). DIP concentrations were the highest at station TYR (17 nmol L^{-1}) and the lowest at the most eastern station (ION, 7 nmol L^{-1}). Consequently, the lowest NO_x:DIP ratio was measured at TYR (0.8), compared to ION and FAST (2.8 and 4.6, respectively). Ammonium concentrations were maximal at TYR (0.045 $\mu mol\ L^{-1}$), intermediate at ION (0.022 $\mu mol\ L^{-1}$), and minimal at FAST (below detection limit). Silicate concentrations were similar at stations TYR and ION (~ 1 $\mu mol\ L^{-1}$) and higher than at station FAST (0.64 $\mu mol\ L^{-1}$).

Very low and similar concentrations of chlorophyll a were measured at the three stations (0.063 - 0.072 $\mu g\ L^{-1}$). The proportion of the different major pigments (Fig. 3) showed that phytoplankton communities at stations TYR and ION were very similar with a dominance of Prymnesiophytes (i.e. 19'-hexanoyloxyfucoxanthin; Ras et al., 2008) followed by Cyanobacteria (i.e. Zeaxanthin; Ras et al., 2008). In contrast, at station FAST, the plankton community was clearly dominated by photosynthetic prokaryotes (i.e. Zeaxanthin and Divinyl-chlorophyll a; Cyanobacteria and Prochlorophytes, respectively; Ras et al., 2008). At all three stations, the proportion of pigments representative of larger species (i.e. Fucoxanthin and Peridinin; diatoms and dinoflagellates respectively; Ras et al., 2008) were very small (< 5% for each pigment).

18

377   Cellular abundances of all studied microorganisms (phytoplankton, micro-grazers,

378   heterotrophic bacteria) were the highest at FAST (Table 2). Picoeukaryotes, *Synechococcus* and

379   heterotrophic prokaryotes abundances followed an east to west increasing trend (ION < TYR <

380   FAST). In contrast, nano-eukaryotes abundance was similar at FAST and ION, and minimal at

381   TYR. The abundance of heterotrophic nanoflagellates (HNF) were similar at TYR and FAST

382   (~110-125 cells mL^{-1}), twice as high as the one observed at station ION. This east to west

383   increasing trend was also observed for micro-phytoplankton and micro-heterotrophs abundances

384   (microscopic analyses; Table 2). The ratio between autotrophic biomass and heterotrophic

385   biomass was clearly in favor of the heterotrophic compartment at stations TYR and FAST (~0.6

386   at the two stations) but the opposite was found at station ION (ca. 1.3).

3.2. Conditions of irradiance, temperature and pH during the experiments

389   Irradiance levels, during the experiments in the control tanks (C1, C2), were maximal at

390   station ION and minimal at station FAST (daily average maximum levels in controls: ~ 1050, ~

391   1130 and ~ 1020 μmol photons m^{-2} s^{-1} at TYR, ION and FAST, respectively; Fig. 4). Decreases

392   of water transparency after dust addition was observed at all three stations with a maximum dust

393   impact at station ION and the lowest impact at station FAST where irradiance levels decreased

394   by only 60 μmol photons m^{-2} s^{-1} after dust addition (average between tanks D and G). At station

395   TYR, a more pronounced decrease was observed in acidified and warmed tanks (G1 and G2)

396   with a decrease of daily average maximum irradiance of ~ 60 and ~ 160 μmol photons m^{-2} s^{-1} as

397   compared to dust-amended tanks D and controls, respectively. Temperature control (Fig. 4) was

398   not optimal showing deviations between replicates of treatment G of up to 1.5 °C (station ION).

399   Temperature in controls and D tanks displayed a daily cycle with an increase during the day and

400 ~~a decrease~~ at night. ~~Overall,~~ the differences between the warmed treatment (G) and the other

401 tanks were +3, +3.2 and +3.6 °C at TYR, ION and FAST, respectively.

402 Addition of CO_2-saturated filtered seawater led to a decrease ~~of~~ pH_T from 8.05 ± 0.004

403 (average $\pm$ SD ~~between~~ C1, C2, D1 and D2 at t0) to 7.74 (average between G1 and G2) at station

404 TYR, from 8.07 ± 0.002 to 7.78 at station ION and 8.05 ± 0.001 to 7.72 at station FAST (Fig. 5).

405 pH_T levels remained more or less constant in ~~ambient pH levels tanks~~ during all three

406 experiments with no clear impact of dust addition ~~in tanks D1 and D2~~. In ~~lowered pH tanks~~, pH

407 levels gradually increased during the experiments with ~~a systematic~~ larger ~~increase in one of the~~

408 duplicate~~s (G1). Yet pH_T~~ increases remained moderate thanks to the flushing of CO_2-enriched air

409 above the tanks (pCO_2 of 1017 ± 11, 983 ± 96, 1023 ± 25 ppm at TYR, ION and FAST,

410 respectively; data not shown). Partial pressure of CO_2 in ambient air was similar ~~at~~ the three

411 stations, ~~i.e. 410 ppm (data not shown). At all three stations,~~ the addition of ^{13}C-bicarbonate ~~to~~

412 ~~all tanks before t0~~ led to an increase of total alkalinity between 6 and 11 μmol kg^{-1} at t0. Dust

413 addition, ~~performed~~ right after t0 in tanks D and G, led to a A_T decrease ~~in these tanks~~ between 8

414 and 16 μmol kg^{-1} at t24h with no apparent effects of warming and acidification. Overall, no large

415 changes in ~~this parameter~~ were observed during the experiments (Fig. 5).

3.3. Changes in nutrient concentrations

417 Dust addition ~~in tanks D and G~~ led to a rapid ~~and maximum~~ input of NO_x (as observed

418 during the first 6 h; Fig. 6; Table 3) ~~of ~ 11 μmol L^{-1}~~ at all three stations with no differences

419 between ~~both~~ treatments. The corresponding dissolution ~~percentage~~ of N ~~contained in the~~ dust

420 ~~analog was~~ between 94 and 99%. In contrast, maximum DIP release ~~(within 6 h after dust~~

421 ~~addition) from the dust analog~~ was much smaller ~~and comprised~~ between 20 and 37 nmol L^{-1},

422 with slightly higher ~~release~~ at FAST (31-37 nmol L^{-1}) as compared to the other stations.

423 Dissolution ~~percentages~~ for DIP ~~were estimated between~~ 9.2 ~~and~~ 17.3% of total phosphorus

424 contained in dust. As a consequence ~~of these contrasted dissolution of N and P~~, NO_x:DIP ratios

425 increased from initial values below 5 to above 300, within 6 h after dust seeding, in ~~the dust~~

426 ~~amended (~~D and G~~) tanks~~ (Fig. 6).

427   After the~~se~~ rapid increases ~~due to~~ N and P ~~releases in dust amended tanks~~, both ~~variables~~

428 decreased with time. While nutrient variability was small in control tanks ~~over the duration of the~~

429 ~~experiments~~ (NO_x and DIP variations below 20 and 3 nmol L^{-1}, respectively), large decrease ~~of~~

430 both elements ~~was measured~~ in dust amended tanks (D and G; Table 4). ~~For NO_x,~~ similar linear

431 decrease~~s~~ were observed throughout the experiments at stations TYR and ION with no visible

432 differences between tanks D and G. In contrast, at station FAST, a more pronounced decrease in

433 NO_x was observed in dust-amended (D and G) tanks ~~as compared to the other stations, with~~

434 ~~detectable larger decreases~~ in warmed and acidified tanks relative to the D treatment.

435 Nevertheless, at all stations, NO_x concentrations in D and G treatments remained far above

436 ambient levels throughout the experiments (> 9 μmol L^{-1}). Abrupt decreases in DIP were

437 observed during the three experiments after the initial increase. At station TYR, after 24 h, all

438 DIP released from dust decreased to initial levels in tanks G while it took two more days to reach

439 initial levels in tanks D. In contrast, at station ION, no clear difference in DIP dynamics was

440 observed between treatments D and G, with concentrations that decreased rapidly during the first

441 24 h but ~~that~~ remained above initial levels until the end of the experiment. At station FAST,

442 similarly to station TYR, DIP decreased rapidly from t12h in treatment G, reaching levels close

443 to initial conditions at the end of the experiment. DIP decrease was much lower in treatment D

444 (Table 4) with concentrations maintained far above ambient levels throughout the experiment.

445 As a consequence of the~~se~~ differences between NO_x and DIP dynamics as well as differences

446 among stations, NO_x:DIP ratio increased ~~during the experiments~~ with clear differences between

447 stations (Fig. 6) and remained much higher than ~~that~~ in the controls ~~over the duration of the three~~

448 ~~experiments~~.

449   Silicate ~~dynamics showed at all stations higher~~ concentrations in dust amended ~~(D and G)~~

450   tanks relative to the controls. At TYR, while concentrations remained stable in control tanks,

451   they increased linearly with time in the other tanks (D and G) with no apparent effect of the

452   imposed increase in temperature and decrease in pH (i.e. tanks G). Difference ~~of~~ $Si(OH)_4$

453   concentration between dust amended treatments (D and G) and controls was ~0.1 µmol L^{-1} at the

454   end of the experiment. At station ION, after an initial decrease ~~of~~ concentrations between t-12h

455   and t0, concentrations increased in all tanks until the end of the experiment with higher

456   ~~concentration~~ in dust amended tanks (D and G) than in controls (no difference between D and G

457   treatments). In contrast, at FAST, concentrations increased ~~between~~ t-12h ~~and t0, and continued~~

458   ~~to increase in all tanks (with higher values in dust amended tanks) until~~ t48h and ~~then~~ decreased

459   until the end of the experiment. At the end of the experiment (t96h), $Si(OH)_4$ concentration was

460   higher in the G treatment than in the D treatment which ~~was~~ similar to the controls.

3.4. Changes in biological stocks

462   ~~Regarding biological stocks,~~ temporal dynamics showed very different patterns ~~amongst~~

463   ~~the three studied~~ stations. At TYR, total chlorophyll *a* concentrations did not change in dust

464   amended tanks ~~maintained under ambient levels of temperature and pH~~ (Fig. 7) and even led to

465   slightly decreased values 24 h after dust addition (e.g. -35 to -38% in D1 and D2, respectively as

466   compared to controls; ~~Table 5~~). No clear effect of dust addition (tanks D vs. C) were detectable

467   for all groups based on pigment analyses (Fig. 7). Results obtained based on flow cytometry

468   ~~counting~~ (Fig. 8) were coherent with these observations and showed stronger decreases in cell

469   abundances for < 20 µm autotrophic groups in tanks D1 and D2 (-77 to -80%). In contrast, ~~at this~~

470   ~~station~~, the abundance of heterotrophic prokaryotes (HP) increased rapidly after dust addition

471   both under ambient (+53-68%) and future (+68%) environmental conditions, with no clear

472   difference among ~~those~~ treatments. In warmed and acidified tanks, strong discrepancies between

473   the duplicates were observed for pigments and autotrophic cell abundances~~, Indeed,~~ tank G1

474   showed ~~moderately higher levels~~ for all variables ~~as compared to tanks C~~ with the exception of

475   pico-eukaryotes, while in G2 all variables responded strongly to dust addition with maximum

476   relative changes of > 300% (with the exception of nano-eukaryotes~~: +119%~~). While HNF

477   abundances responded positively to the treatments in D1, D2 and G2 (~~+100-352%~~), abundances

478   increased sharply in tank G1 towards the end of the experiment (~~+1095%~~).

479   At ION, ~~a~~ clear ~~distinction~~ between treatments ~~could be~~ observed for almost all pigments

480   and cell abundances (Fig. 7, Fig. 8). With the exception of nano-eukaryotes and HNF, all

481   variables (pigments and cell abundances) increased as a response to both dust addition and

482   warmed/acidified conditions ~~(i.e. C < D < G). As an example~~ (Table 5), the maximum relative

483   changes as compared to controls observed for total chlorophyll *a* were 109-183% and 399-426%

484   in tanks D and G, respectively. The highest stimulation ~~to~~ dust addition was observed for

485   *Synechococcus* with a +317-390% ~~increase~~ and +805-1425% increase in D and G tanks

486   respectively (Table 5). ~~Abundances of~~ nano-eukaryotes and HNF ~~suggested~~ no impact of dust

487   addition under ambient conditions but a ~~positive impact~~ in treatment G. In contrast to ~~what was~~

488   ~~observed~~ at TYR ~~for HP abundances, an effect of~~ temperature and pH ~~was observed~~ at station

489   ION with a higher impact of dust addition under future environmental conditions.

490   At station FAST, all ~~above mentioned variables related to~~ biological stocks increased

491   strongly after dust addition (Fig. 7, Fig. 8 and Table 5). ~~For instance,~~ total chlorophyll *a*

492   increased ~~following an exponential trend~~ until the end of the experiment ~~reaching maximal~~

493   ~~values at t96h~~ with slightly lower values observed under ambient environmental conditions

494   (+237-318% in D tanks ~~vs.~~ ~ +400% in G tanks). Prymnesiophytes (i.e. 19'-

495   hexanoyloxyfucoxanthin) and diatoms (i.e. Fucoxanthin) appeared as the groups benefiting the

496   most from dust addition with no large impacts of warming/acidification. ~~In contrast,~~

497   Pelagophytes (i.e. 19'-butanoyloxyfucoxanthin) and green algae (i.e. Total Chlorophyll *b*)

498 ~~responded much more~~ in treatment G ~~than in treatment D~~. Finally, although Cyanobacteria (i.e.

499 Zeaxanthin) responded faster to dust addition under future environmental conditions (tanks G),

500 this effect ~~tended to attenuate~~ towards the end of the experiment. In contrast to estimates based

501 on ~~HPLC data~~, increases in cell abundances did not generally ~~take place~~ until the end of the

502 experiment. While abundances ~~in~~ pico-eukaryotes increased until t96h in treatment D,

503 abundances sharply declined between t72h and t96h for this group in treatment G. The same

504 trend was observed for *Synechococcus* ~~during this experiment~~, although discrepancies between

505 duplicates in treatment D at ~~sampling time~~ t96h did not allow drawing conclusions on the

506 behavior of this group ~~at~~ the end of the experiment. ~~Both under ambient and future conditions~~,

507 abundances of nano-eukaryotes declined sharply between t72h and t96h. The decline in HP

508 abundances ~~appeared even~~ earlier during the experiment with moderate maximum relative

509 differences as compared to controls ~~observed~~ at t48h. HP abundances declined very sharply

510 between t48h and t96h in treatment G, reaching control levels, while this decline was less sharp

511 under ambient ~~environmental levels~~. Finally, HNF dynamics during this experiment was hard to

512 ~~evaluate with no clear effects of dust addition or pH/temperature conditions and with a~~ large

513 increase in abundances in only one duplicate of treatment G (t24h) followed by a gradual

514 ~~decrease~~.

515   Abundances of meso-zooplankton at the end of the experiments showed relatively similar

516 values at stations TYR and ION while much higher levels were observed at station FAST (Fig.

517 9). As a consequence of large variability between duplicates at stations TYR and ION, no clear

518 effects of treatments were detected. At station FAST, although the sample size was too low to

519 statistically test for differences, higher total abundances of meso-zooplankton species were

520 observed in the dust-amended tanks with no differences between ambient and future conditions

521 of temperature and pH. However, differences in abundance were visible between these two

522   treatments for specific groups, with respectively higher abundance of Harosa and lower

523   abundance of Crustacea (other than copepods) and Mollusca in warmed and acidified tanks.

4. Discussion

4.1. Initial conditions

Over the transect, the mixed layer occupied the first 20 m. It was shallower at TYR as compared to ION and FAST (mixed layer depth, MLD of ~ 10 vs ~15 m, respectively) at the time of the sampling (Van Wambeke et al., 2020a). Such shallow MLD is well representative of stratified conditions encountered in the western Mediterranean basin in late spring/early summer (D'Ortenzio et al., 2005). Overall, the three experiments were conducted with surface seawater collected during oligotrophic conditions typical of the open Mediterranean Sea at this period of the year (late spring). Although direct measurements of NO_x and DIP concentrations using nanomolar techniques (as performed in our study) are scarce in the Mediterranean Sea, the low levels measured during the cruise are in agreement with DIP values reported for the three studied basins (Djaoudi et al., 2018) and with NO_x and DIP concentrations measured in coastal waters of Corsica in late spring/early summer (Louis et al., 2017b; Pulido-Villena et al., 2014; Ridame et al., 2014). Furthermore, at all three stations, NO_x:DIP molar ratios in the tested surface waters were well below the Redfield ratio (16:1) and are consistent with ratios found in these previously cited studies. Both low NO_x:DIP ratio and low nutrient concentrations suggest that communities found at the three stations experienced N and P co-limitation at the start of the experiments, as previously shown by Tanaka et al. (2011). A side nutrient enrichment experiment confirmed that, at the three sites, heterotrophic bacteria were mainly N-P co-limited (Van Wambeke et al., 2020b). In contrast to N and P, initial concentrations of dissolved Fe in the sampled seawater, ranging from 1.5 nmol L^{-1} at TYR to 2.5 nmol L^{-1} at ION (Roy-Barman et al., 2020), were unlikely limiting for biological activity as previously shown in the Mediterranean Sea under stratified conditions (Bonnet et al., 2005; Ridame et al., 2014).

547   Low total chlorophyll *a* concentrations in ~~the tested~~ waters were ~~representative of surface~~

548   ~~concentrations reported~~ for the Western and Central Mediterranean Sea in late spring/early

549   summer, ~~both from~~ remote sensing ~~images~~ (Bosc et al., 2004), and from *in situ* measurements

550   ~~provided in a database from~~ Manca et al. (2004). While large species (i.e. diatoms,

551   dinoflagellates) represented only ~10% of the total chlorophyll *a* biomass ~~of the tested waters,~~

552   the composition of the smaller size phytoplankton communities differed substantially. ~~Indeed,~~

553   ~~communities were clearly dominated by~~ nano-eukaryotes at stations TYR and ION and a larger

554   contribution from pico-eukaryotes and Cyanobacteria ~~was observed~~ at station FAST. Due to their

555   low competitiveness under nutrient limitation, the small contribution of large phytoplankton cells

556   at the start of the experiment is a fingerprint of LNLC areas in general, and of surface

557   Mediterranean waters in late spring and summer (Siokou-Frangou et al., 2010).

558   ~~As~~ biomass of both heterotrophic nanoflagellates and prokaryotes followed a west to east

559   gradient (FAST > TYR > ION), ~~the ratio of autotrophic vs~~ heterotrophic ~~biomass appeared~~

560   ~~clearly in favor of the heterotrophic compartment~~ at stations TYR and FAST (~~ratio of 0.6~~) while

561   ~~a value above 1 was estimated~~ at ION (~~ratio of 1.3). This is coherent with the highest~~ net

562   community production (NCP) rates ~~being reported at this station by~~ Gazeau et al. (2021)

563   show~~ing that the~~ initial community ~~at the start of this experiment was very~~ close to metabolic

564   balance (mean $\pm$ SE: -0.06 $\pm$ 0.09 μmol O$_2$ L^{-1} d^{-1}). ~~The~~ highest community respiration rates and

565   consequently lowest NCP rates ~~were measur~~ed at station TYR (-1.9 μmol O$_2$ L^{-1} d^{-1}) ~~further~~

566   suggesting that the autotrophic plankton community was not very active and ~~relying~~ on

567   regenerated nutrients, as shown by the high~~est~~ level of NH$_4^+$ ~~measured~~ at the start of ~~this~~

568   experiment. In contrast, although slightly heterotrophic (Gazeau et al., 2021) and limited by the

569   low amount of nutrients, the community ~~of the tested waters~~ at FAST ~~was the most active as~~

570   ~~shown by~~ the highest levels of ^{14}C production and heterotrophic prokaryote production (Gazeau

571   et al., 2021) as well as N$_2$ fixation (Céline Ridame, unpublished results). Altogether, the

heterotrophic signature of the three investigated stations, although closer to metabolic balance at
ION, reflected typical biogeochemical conditions in the Mediterranean Sea during late spring to
early summer (Regaudie-de-Gioux et al., 2009).

4.2. Critical assessment of the experimental system and methodology

The experimental tanks used in this study have been successfully validated in previous
studies designed to investigate the inputs of macro- and micro-nutrients (e.g. NO_x, DIP, DFe)
and the export of organic matter, ~~under close-to-abiotic conditions (seawater filtration onto~~ 0.2
μm) following simulated wet dust events using the same analog as used in our study (Bressac
and Guieu, 2013; Louis et al., 2017a, 2018). Louis et al. (2017a, 2018) further investigated these
impacts under lowered pH conditions, ~~although no control of atmospheric~~ pCO_2 ~~was performed~~
resulting in a rapid increase of pH levels in the acidified filtered seawater due to CO_2 outgassing
(from ~7.4 to ~7.7 in six days). ~~Since those above-mentioned studies, in order to avoid this, we~~
~~improved~~ our experimental system ~~to allow mimicking future conditions by controlling~~
atmospheric pCO_2 in addition to light and temperature (i.e. climate reactors). ~~This allowed to~~
significantly reduce CO_2 outgassing and maintain pH levels close to ~~experimental~~ targets. ~~Still,~~
~~as illustrated in Fig. 5, the~~ regulation of atmospheric CO_2 was consistently more efficient in tank
G2 compared to G1, resulting in a small discrepancy in terms of pH (highest difference of 0.04
pH units between the two G tanks at FAST), possibly due to a potential leak or a longer flushing
time above tank G1. Nevertheless, as no systematic differences in ~~terms of~~ biological response
were observed between these two tanks, ~~we believe that~~ these small differences in ~~terms of~~
~~regulated~~ pH had no ~~consequences~~ on the obtained results.

The lids above tanks, equipped with LEDs in order to reproduce sunlight intensity and
spectrum, were used for the first time during these experiments. While simulated intensities were

close to estimates for the Northwestern Mediterranean Sea at 5 m depth in June (~1100 μmol photons m^{-2} s^{-1}; Bernard Gentili, personal communication, 2017) and fairly consistent between duplicates under control and dust-amended conditions, larger differences were observed between ~~the two warmed and acidified tanks. The reasons of~~ these discrepancies could result from small differences ~~in terms of light intensity regulation between lids, of~~ PAR sensors calibration and/or of different turbidity related to the amount of particles remaining in the tanks. As for pH ~~discussed above,~~ replication in terms of biological response appeared satisfactory ~~for this treatment~~ (except at station TYR; see ~~below), and we believe these technical issues had no significant impacts on our results~~.

Continuous measurements in the tanks showed that temperature was not spatially homogeneous, leading to significant differences among replicates. This was ~~especially the case~~ for warmed tanks (treatment G) ~~for which~~ a maximal average difference over the experimental period of 0.7 °C ~~was observed~~ during the FAST experiment. ~~As for the other controlled parameters discussed above,~~ these discrepancies did not systematically lead to observable differences in the investigated stocks and processes between duplicates (except at TYR, see below).

The ~~relatively low number of experimental units that could be installed inside an embarkable~~ clean container ~~restrained~~ our possibility to ~~consider more than two~~ replicates ~~per~~ treatment. ~~Fortunately, as already said,~~ differences between duplicates were, for the vast majority of studied variables and processes, lower than differences between treatments and appear ~~acceptable~~ considering the difficulty to incubate plankton communities for which slight differences in ~~their~~ initial composition can translate into ~~very~~ important differences in dynamics (Eggers et al., 2014). Nevertheless, ~~we have to note that~~ important discrepancies were detected ~~regarding~~ autotrophic stocks and processes (Gazeau et al., 2021) for ~~tanks of~~ the warmed and acidified treatment at station TYR. The reasons behind these differences are ~~not fully understood~~

621 ~~but we strongly suspect that~~ heterotrophic nano-flagellates~~, feeding mainly~~ on prokaryotic

622 picoplankton (Sherr and Sherr, 1994), ~~exerted a strong top-down control on this group~~ in tank G1

623 ~~in which~~ HNF abundance sharply increased during the experiment. ~~All in all~~, while the

624 methodology used in this study allowed to successfully evaluate the impacts of dust addition

625 under both present and future environmental conditions at two out of three tested waters, the~~se~~

626 discrepancies at station TYR prevent us from drawing any strong conclusion on the effect of dust

627 addition on the dynamics of the community under future environmental conditions at that station.

4.3. Impact of dust addition under present environmental conditions

630 During ~~the three~~ experiments, the observed increases in NO_x and DIP few hours after

631 dust addition under present environmental conditions were ~~rather~~ similar to the enrichment ~~levels~~

632 obtained during the DUNE experiments ~~at~~ the surface of the mesocosms (~ 50 m^3) after the

633 simulation of a wet dust deposition using the same dust analog and the same simulated flux

634 (Pulido-Villena et al., 2014; Ridame et al., 2014). The intensity of ~~this~~ simulated wet deposition

635 event (i.e. 10 g m^{-2}) represents a high but realistic scenario, as several studies reported even

636 higher short wet deposition events in this area of the Mediterranean Sea (Bonnet and Guieu,

637 2006; Loÿe-Pilot and Martin, 1996; Ternon et al., 2010). Furthermore, based on previous studies

638 reporting the mixing between dust and polluted air masses during the atmospheric transport of

639 dust particles (e.g. Falkovich et al., 2001; Putaud et al., 2004), we ~~chose to use an~~ evapo-

640 condensed dust analog that mimics the processes taking place in the atmosphere prior to

641 deposition, essentially the adsorption of inorganic and organic soluble species (e.g. sulfate and

642 nitrate; see Guieu et al., 2010a, for further details). The imposed evapo-condensation processes

643 are responsible for the large nitrate releasing capacity of the dust particles used in our study. As a

644 consequence, the addition of new nutrients from dust in our study and during the P and R DUNE

experiments were much higher, especially for NO_x, than those observed by Pitta et al. (2017, and

references therein) and Ridame et al. (2014) following the simulation of a dry Saharan dust

deposition event. This confirms that wet dust deposition is a more efficient source of

bioavailable nutrients ~~compared to~~ dry dust deposition.

Although NO_x and DIP increases after dust addition were ~~rather~~ similar ~~during our three~~

experiments, the subsequent dynamics of these elements and the impacts on plankton community

composition and functioning were drastically different. While NO_x levels decreased moderately

over the course of our experiments due to biological uptake, more abrupt decreases were

observed for DIP released by dust, reaching values close to the ones observed in the controls,

except at station FAST where concentrations were still above ambient levels at the end of the

experiment.

~~Regarding biological stocks, most~~ experiments ~~reporting~~ on the effect of dust addition in

the Mediterranean Sea showed significant increases in chlorophyll *a* concentrations (mean ~90%

increase; Guieu and Ridame, 2020). Interestingly, no stimulation of autotrophic biomass and

primary production rates (Gazeau et al., 2021) was observed in dust-amended tanks under

present conditions at station TYR. To the best of our knowledge, this is the first experimental

evidence of a complete absence of response from an autotrophic community following dust wet

deposition. The absence of response from autotrophic stocks could be due to a tight top-down

control ~~from~~ grazers hiding potential responses from the autotrophic community (Lekunberri et

al., 2010; Marañón et al., 2010) and/or a competition for ~~nutritive resources~~ with heterotrophic

prokaryotes (Marañón et al., 2010). ~~Regarding the first hypothesis,~~ Feliú et al. (2020) have

shown that the mesozooplankton assemblage at TYR was clearly impacted by a dust event that

took place nine days before sampling at that station as evidenced from particulate inventory of

lithogenic proxies (Al, Fe) in the water column (Bressac et al., in preparation). This dust

deposition likely stimulated phytoplankton growth and consequently increased the abundance of

670 herbivorous grazers (copepods) and attracted carnivorous species. ~~With respect to the second~~

671 ~~hypothesis, it is well known that not only phytoplankton but also~~ heterotrophic bacteria are

672 limited by inorganic nutrients, mainly DIP, in oligotrophic systems (Obernosterer et al., 2003;

673 Van Wambeke et al., 2001). ~~Indeed, many~~ recent studies have shown significant increase in

674 heterotrophic bacterial abundance, respiration and/or production following dust deposition (and

675 nutrient enrichment) in these areas (Lekunberri et al., 2010; Pitta et al., 2017; Pulido-Villena et

676 al., 2008; Romero et al., 2011). ~~Most of the time,~~ heterotrophic ~~processes~~ appear to be more

677 stimulated ~~by dust pulses compared to~~ autotrophic ~~processes~~ with increasing degree of

678 oligotrophy, ~~the dominant response being~~ modulated by the competition for nutrients between

679 phytoplankton and bacteria (Marañón et al., 2010). This ~~is clearly what was observed at this~~

680 ~~station,~~ with heterotrophic prokaryotes reacting quickly and strongly to nutrient addition both in

681 terms of abundances and production rates (Gazeau et al., 2021). These two aforementioned

682 hypotheses are not mutually exclusive, and the quick response of heterotrophic prokaryotes to

683 dust addition is coherent with the ~~strongest~~ net heterotrophy ~~of the tested waters~~ at this station

684 (see 4.1). ~~The strong stimulation of heterotrophic prokaryotes and the absence of detectable~~

685 ~~effects on the autotrophic compartment drove the community towards an even stronger net~~

686 ~~heterotrophic state as illustrated by the decrease in the autotrophic to heterotrophic biomass ratio~~

687 ~~following dust addition (data not shown). This was further shown by~~ increases in community

688 respiration and decreases in net community production rates in dust-amended as compared to

689 control tanks (Gazeau et al., 2021) ~~and suggest that~~ dust addition to surface waters strongly

690 dominated by heterotrophs leads to a reduction of the capacity of these ~~waters~~ to export organic

691 matter and sequester atmospheric CO_2.

692 In contrast to ~~what was observed~~ at TYR, ~~fertilization~~ of primary producers was observed at

693 stations ION and FAST under present conditions with overall ~~relative changes much~~ higher than

694 ~~from~~ previous studies compiled by Guieu and Ridame (2020). The largest increase in chlorophyll

a concentrations at station FAST is coherent with ~~the largest~~ NO$_x$ decrease observed ~~in our~~

~~study, which occurred~~ at this station. Interestingly, ~~following dust addition at this station,~~

~~autotrophic production did not lead to DIP exhaustion throughout the experiment as~~ DIP

concentrations were still above ambient conditions at the end of the experiment. Maxim~~al~~

primary production rates (^{14}C-incorporation) ~~at this station~~ at the end of the experiment suggest ~~a~~

strong DIP recycling and the dominance of regenerated production towards the end of the

experiment (Gazeau et al., 2021). Although, in some cases, *Synechococcus* appeared stimulated

by dust addition (Herut et al., 2005; Lagaria et al., 2017; Paytan et al., 2009), Guieu et al.

(2014b) showed that, based on the analysis of several aerosols addition studies, this group had

generally weak responses to aerosol addition in contrast to nano- and micro-phytoplankton,

suggesting that aerosol deposition may lead to an increase in larger ~~size class~~ phytoplankton.

Yet, at stations ION and FAST, the increase in *Synechococcus* abundance in dust-amended tanks

was the highest relative to those of pico- and nano-eukaryotes. ~~This was especially true~~ at station

ION ~~where~~ no clear response to nutrient enrichment was observed for nano-eukaryotes

throughout the experiment. However, it must be stressed that our experiments were ~~performed~~

~~over a~~ relatively short period (3 to 4 days)~~, and~~ the sharp increase in Fucoxanthin paralleled by a

decrease in silica~~tes~~, at the end of the experiment at station FAST where DIP limitation was not

yet apparent, suggests a delayed response of diatoms as compared to smaller ~~groups (i.e.~~

~~autotrophic prokaryotes, pico- and nano-eukaryotes). Although this was not observed based on~~

~~pigment analyses,~~ the sharp decline in nano-eukaryote abundances in dust-amended tanks at the

end of the FAST experiment, further suggests that this group, react~~ing~~ quickly to nutrient

enrichment was progressively grazed and/or outcompeted by larger phytoplankton species.

~~In contrast to what was observed at TYR, at station FAST, the competition for nutrients~~

~~between autotrophs and heterotrophs was clearly in favor of autotrophs with a clear increase in~~

~~the ratio between autotrophic and heterotrophic biomass reaching values of up to 4 (data not~~

shown). While, ~~as discussed above,~~ all groups of primary producers benefited from nutrient enrichment at ~~this station,~~ the increases in heterotrophic prokaryote abundances were ~~rather limited following dust deposition,~~ leading to an increase of net community production rates throughout th~~is~~ experiment ~~to reach~~ positive levels while control tanks remained below metabolic balance (Gazeau et al., 2021). At station ION, the situation was ~~somewhat~~ intermediate with a similar enhancement of both autotrophic and heterotrophic stocks and no clear changes in the ratio between autotrophic and heterotrophic biomass (data not shown), although the system ~~appeared in favor of~~ net autotrophy at the end of the experiment in dust - amended tanks under present environmental conditions (Gazeau et al., 2021).

Transfer of newly produced organic matter to higher trophic levels in the different treatments was ~~evaluated~~ through the quantification of meso-zooplankton abundance at the end of each experiment. ~~Although we are fully aware that such an approach is certainly criticizable considering the low incubation times (3 to 4 days), it may still be representative of lowered mortality or faster growth.~~ Altogether it ~~does not appear as a surprise~~ that an increase in meso-zooplankton abundances was only detected at station FAST where the strongest enhancement of primary production was observed. Such an increase in meso-zooplankton abundance in the dust-amended as compared to control treatment was observed during land-based mesocosm experiments in the Eastern Mediterranean Sea (Pitta et al., 2017).

Finally, although no clear effects of dust deposition under present conditions were detectable on autotrophic prokaryotes at station TYR, the strongest increase in N_2 fixation rates was recorded at this station (Céline Ridame, unpublished results). However, the potential impact of this process on NO_x concentration is ~~highly~~ negligible compared to the very large stock of NO_x present in the dust-amended tanks, as less than 1 nmol L^{-1} d^{-1} of NO_x ~~can be produced by this process~~ (Céline Ridame, unpublished results).

34

4.4. Impact of dust addition under future environmental conditions

Very few past studies have investigated the release and fate of nutrients from atmospheric particles under climate conditions as expected for the end of the century, and, to the best of our knowledge, our study represents the first attempt to test for the combined effect of ocean warming and acidification on these processes. Louis et al. (2018) have already shown from an experiment performed under close-to-abiotic conditions (seawater filtration onto 0.2 μm) that even an extreme ocean acidification scenario ($\sim$ -0.6 pH units) does not impact the bioavailability of macro- and micro-nutrients (NO_x, DIP and DFe) from dust addition for surface phytoplankton communities in the oligotrophic Northwestern Mediterranean Sea, using the same dust analog and simulated flux as used during our experiments. Similar results were presented by Mélançon et al. (2016) regarding the release of DFe from dust in high-nutrient low-chlorophyll (HNLC) waters of the Northeastern Pacific, following a mild ocean acidification scenario of -0.2 pH units. As no differences were observed for NO_x and DIP concentrations within few hours following dust addition under present and future environmental conditions, our results agree with these previous findings and further highlights the absence of direct effect of ocean warming (+3 °C) on the release of nutrients from atmospheric particles.

In contrast, following these similar nutrient releases, different nutrient consumption dynamics were observed between ambient and warmed/acidified tanks. These differences were substantially dependent on the considered nutrient and investigated station. Regarding NO_x, no impacts of warming and acidification could be observed at stations TYR and ION due to low net decreasing rates compared to the large increase following dust addition. In contrast, at the most productive station FAST, as a consequence of strongly enhanced biological stocks (see

767 thereafter) and metabolic rates (Gazeau et al., 2021)~~.~~ larger NO$_x$ consumption rates were shown

768 under future environmental conditions.

769   The differences in DIP dynamics between the two dust-amended treatments were more

770 complex to interpret ~~depending on the investigated station.~~ A clear feature of our experiments is

771 that, in contrast to present day pH and temperature conditions, all the stock of DIP released from

772 dust was consumed at the end of the three experiments under future conditions, ~~suggesting a~~

773 ~~much faster consumption by autotrophs and heterotrophic prokaryotes. That being said,~~ the rate

774 of decrease ~~under future environmental conditions~~ differed depending on the station. While DIP

775 dynamics were quite similar between tanks maintained under present and future environmental

776 conditions at ION, warming and acidification induced a faster decrease of DIP at TYR and

777 FAST, with a full consumption of the released DIP within 24 h. An interesting outcome at station

778 TYR was that, despite the important discrepancies observed for autotrophic stocks and metabolic

779 rates between the duplicates G1 and G2 (see section 4.2), a ~~very~~ similar dynamics was observed

780 for DIP concentrations in these tanks. As heterotrophic prokaryote biomass and production rates

781 (Gazeau et al., 2021) did not differ between these duplicate tanks, this further highlights the clear

782 dominance of heterotrophic processes at this station, a dominance which was exacerbated by dust

783 addition under future environmental conditions, leading to an even stronger heterotrophic state at

784 the end of this experiment (Gazeau et al., 2021).

785   At station ION, large impacts of warming and acidification ~~have been observed,~~

786 ~~especially for primary producers, as shown by almost doubled~~ chlorophyll *a* concentrations ~~as~~

787 ~~compared to~~ dust amended tanks ~~(D)~~. At this station, all autotrophic groups ~~benefited from~~ ocean

788 acidification and warming. *Synechococcus* and to a lesser extent pico-eukaryotes ~~appeared as the~~

789 ~~most impacted ones.~~ Yet these differences ~~of sensitivity among autotrophs~~ did not lead to

790 ~~detectable~~ changes in the composition of the autotrophic assemblage ~~as compared to ambient~~

791 ~~conditions,~~ with ~~still a large dominance of~~ nano-eukaryote carbon biomass at the end of this

experiment (62% in treatment G vs. 64% in treatment D). ~~Interestingly,~~ although the ratio

between autotrophic and heterotrophic biomass appeared impacted ~~positively~~ under future

environmental conditions, reaching values of up to 2 at the end of this experiment ~~(data not~~

~~shown)~~, warming and acidification led to a decrease in net community production (Gazeau et al.,

2021) suggesting that in the coming decades the capacity of surface seawater to sequester

anthropogenic CO_2 will be lowered.

Similarly, at FAST, all phytoplankton groups were impacted positively by warming and

acidification with the strongest changes detected for *Synechococcus* as compared to present

environmental conditions. However, in contrast to station ION, all groups reached maximal

abundances (and carbon biomass) after 3 days of incubations, thereafter drastically decreasing

most likely as a consequence of DIP limitation (see above). It must be stressed that this pattern

could not be observed ~~through~~ pigment ~~dynami~~es as no ~~sampling was performed~~ for these

analyses after 3 days of incubation. Also, in contrast to station ION, the abundance of

heterotrophic prokaryotes in the warmer and acidified treatment reached a maximum after 2 days

of incubations and then ~~strongly~~ decreased to reach levels observed in the control treatment. This

suggests that ~~the~~ heterotrophic ~~compartment was~~ the first to suffer from DIP limitation and

further highlights the dominance of ~~the autotrophic compartment~~ in terms of nutrient

consumption at this station. ~~As observed at station ION,~~ although the ratio between autotrophic

and heterotrophic biomass increased under future environmental conditions, Gazeau et al. (2021)

reported on a decrease in net community production rates in this treatment as compared to

ambient environmental conditions, suggesting that, in the future, nutrient release from dust will

lead to a lesser sequestration capacity of surface waters for atmospheric CO_2.

The~~se~~ positive effects of warming and acidification on the abundance of phytoplankton ~~cells,~~

~~especially for small species~~, as observed at ION and FAST are in line with previously published

studies. ~~Indeed,~~ although ~~very contrasted results have been shown on~~ the effect of ocean

817   acidification on small autotrophic species (e.g. Dutkiewicz et al., 2015), there is increasing

818   evidence that small phytoplankton species will be favored in a warmer ocean (e.g. Chen et al.,

819   2014; Daufresne et al., 2009; Morán et al., 2010). ~~As mentioned earlier,~~ our experimental

820   protocol was not conceived to discriminate temperature from pH effects, however results concur

821   with those of Maugendre et al. (2015) which further suggested temperature over elevated CO_2 as

822   the main driver of increased picophytoplankton abundance in the Mediterranean Sea.

823   These enhanced fertilizing effects on primary producers at ION and FAST, under future

824   as compared to present environmental conditions, did not seem to reach higher trophic levels as

825   no clear differences in meso-zooplankton abundances were observed between ambient and

826   warmed/acidified tanks at the end of the experiments. ~~We fully acknowledge that~~ the duration of

827   our experiments was ~~certainly~~ too short to carefully assess the proportion of newly formed

828   organic matter consumed by meso-zooplankton species and its effect on their ~~abundances,~~ yet

829   group-specific variations were observed. ~~Similarly,~~ Gazeau et al. (2021) did not observe an

830   additional impact of future environmental conditions on the export of organic matter after dust

831   addition.

5. Conclusion

These experiments conducted during the PEACETIME cruise represent the first attempt to investigate the impacts of atmospheric deposition on surface plankton communities both under present and future environmental conditions. Despite few experimental issues ~~that are discussed~~, the three experiments provided new insights on these potential impacts in the open Mediterranean Sea. ~~Interestingly, the effect of dust deposition was highly different~~ between the three investigated stations in the Tyrrhenian Sea, Ionian Sea and in the Algerian basin. ~~As~~ the initial conditions ~~in the sampled surface seawater~~ at the three stations were very similar in terms of nutrient ~~availability~~ and chlorophyll ~~content~~, these differences ~~rather~~ seem to be a consequence of the initial metabolic states of the community (autotrophy vs. heterotrophy). In all three cases, nutrient addition from dust deposition did not strongly modify but rather exacerbated this initial state. Relative changes in main parameters presented in this manuscript and processes presented in Gazeau et al. (2021) as a consequence of dust addition under present and future environmental conditions are shown in Fig. 10, and compared to the compilation of published data for the Mediterranean Sea from Guieu and Ridame (2020). At station TYR, under conditions of a clear dominance of heterotrophs on the use of resources and potentially a higher top-down control from grazers, dust addition drove the community into an even more heterotrophic state with no detectable effect on primary producers. At station ION, where the community was initially closer to metabolic balance, both heterotrophic and autotrophic compartments benefited from dust derived nutrients. At FAST, the ~~most active~~ station ~~in terms of~~ autotrophic production, addition of nutrients ~~boosted~~ both compartments but heterotrophic prokaryotes became quickly P-limited and overall larger effects were observed for phytoplankton. Ocean acidification and warming did not have any detectable impact on the release of nutrients from atmospheric particles. Furthermore, these external drivers did not

856   drastically modify the composition of the autotrophic assemblage with all groups benefiting from

857   warmer and acidified conditions. However, although for two out of the three stations

858   investigated, larger increases were observed for autotrophic as compared to heterotrophic stocks

859   under future environmental conditions, a stronger impact of warming and acidification on

860   mineralization processes (Gazeau et al., 2021) suggests that, in the future, the plankton

861   communities of Mediterranean surface waters will have a decreased capacity to sequester

862   atmospheric CO_2 following the deposition of atmospheric particles.

Data availability

All data and metadata will be made available at the French INSU/CNRS LEFE CYBER database (scientific coordinator: Hervé Claustre; data manager, webmaster: Catherine Schmechtig). INSU/CNRS LEFE CYBER (2020)

Author contributions

FG and CG designed and supervised the study. FG, CG, CR and KD sampled seawater from the experimental tanks during the experiments. JMG and GDL participated in the technical preparation of the experimental system and all authors participated in sample analyses. FG, CR and CG wrote the paper with contributions from all authors.

Financial support

Acknowledgments

References

Aminot, A. and Kérouel, R.: Dosage automatique des nutriments dans les eaux marines : méthodes en flux continu, Editions Ifremer, méthodes d'analyse en milieu marin., 2007.

Behrenfeld, M. J., O'Malley, R. T., Siegel, D. A., McClain, C. R., Sarmiento, J. L., Feldman, G. C., Milligan, A. J., Falkowski, P. G., Letelier, R. M. and Boss, E. S.: Climate-driven trends in contemporary ocean productivity, Nature, 444(7120), 752–755, 2006.

Bergametti, Gi., Dutot, A.-L., Buat-Ménard, P., Losno, R. and Remoudaki, E.: Seasonal variability of the elemental composition of atmospheric aerosol particles over the Northwestern Mediterranean, Tellus B: Chemical and Physical Meteorology, 41(3), 353–361, https://doi.org/10.3402/tellusb.v41i3.15092, 1989.

Bonnet, S. and Guieu, C.: Atmospheric forcing on the annual iron cycle in the western Mediterranean Sea: A 1-year survey, Journal of Geophysical Research: Oceans, 111(C9), https://doi.org/10.1029/2005JC003213, 2006.

Bonnet, S., Guieu, C., Chiaverini, J., Ras, J. and Stock, A.: Effect of atmospheric nutrients on the autotrophic communities in a low nutrient, low chlorophyll system, Limnology and Oceanography, 50(6), 1810–1819, https://doi.org/10.4319/lo.2005.50.6.1810, 2005.

Børsheim, K. Y. and Bratbak, G.: Cell volume to cell carbon conversion factors for a bacterivorous Monas sp. enriched from seawater, Marine Ecology Progress Series, 36(2), 171–175, 1987.

Bosc, E., Bricaud, A. and Antoine, D.: Seasonal and interannual variability in algal biomass and primary production in the Mediterranean Sea, as derived from 4 years of SeaWiFS observations, Global Biogeochemical Cycles, 18(1), https://doi.org/10.1029/2003GB002034, 2004.

Bressac, M. and Guieu, C.: Post-depositional processes: What really happens to new atmospheric iron in the ocean's surface?, Global Biogeochemical Cycles, 27(3), 859–870, https://doi.org/10.1002/gbc.20076, 2013.

913   Bressac, M., Wagener, T., Tovar-Sanchez, A., Ridame, C., Albani, S., Fu, F., Desboeufs, K. and

914   Guieu, C.: Residence time of dissolved and particulate trace elements in the surface

915   Mediterranean Sea (Peacetime cruise), Biogeosciences, in preparation.

916   Bressac, M., Guieu, C., Doxaran, D., Bourrin, F., Desboeufs, K., Leblond, N. and Ridame, C.:

917   Quantification of the lithogenic carbon pump following a simulated dust-deposition event

918   in large mesocosms, Biogeosciences, 11(4), 1007–1020, https://doi.org/10.5194/bg-11-

919   1007-2014, 2014.

920   Chen, B., Liu, H., Huang, B. and Wang, J.: Temperature effects on the growth rate of marine

921   picoplankton, Marine Ecology Progress Series, 505, 37–47,

922   https://doi.org/10.3354/meps10773, 2014.

923   Christaki, U., Courties, C., Massana, R., Catala, P., Lebaron, P., Gasol, J. M. and Zubkov, M. V.:

924   Optimized routine flow cytometric enumeration of heterotrophic flagellates using SYBR

925   Green I, Limnology and Oceanography: Methods, 9(8), 329–339,

926   https://doi.org/10.4319/lom.2011.9.329, 2011.

927   Daufresne, M., Lengfellner, K. and Sommer, U.: Global warming benefits the small in aquatic

928   ecosystems, PNAS, 106(31), 12788–12793, https://doi.org/10.1073/pnas.0902080106,

929   2009.

930   Desboeufs, K., Leblond, N., Wagener, T., Bon Nguyen, E. and Guieu, C.: Chemical fate and

931   settling of mineral dust in surface seawater after atmospheric deposition observed from

932   dust seeding experiments in large mesocosms, Biogeosciences, 11(19), 5581–5594,

933   https://doi.org/10.5194/bg-11-5581-2014, 2014.

934   Desboeufs, K., Bon Nguyen, E., Chevaillier, S., Triquet, S. and Dulac, F.: Fluxes and sources of

935   nutrient and trace metal atmospheric deposition in the Northwestern Mediterranean,

936   Atmospheric Chemistry and Physics, 18(19), 14477–14492, https://doi.org/10.5194/acp-

937   18-14477-2018, 2018.

938　Dickson, A. G., Sabine, C. L. and Christian, J. R.: Guide to best practices for ocean CO2

939　　　measurements, PICES, Sydney., 2007.

940　Dinasquet, J., Bigeard, E., Gazeau, F., Marañón, E., Ridame, C., Van Wambeke, F.,

941　　　Obernosterer, I. and Baudoux, A.-C.: Impact of dust enrichment on the microbial food web

942　　　under present and future conditions of pH and temperature, Biogeosciences Discussions,

943　　　2021.

944　Djaoudi, K., Van Wambeke, F., Coppola, L., D'Ortenzio, F., Helias-Nunige, S., Raimbault, P.,

945　　　Taillandier, V., Testor, P., Wagener, T. and Pulido-Villena, E.: Sensitive Determination of

946　　　the Dissolved Phosphate Pool for an Improved Resolution of Its Vertical Variability in the

947　　　Surface Layer: New Views in the P-Depleted Mediterranean Sea, Front. Mar. Sci., 5,

948　　　https://doi.org/10.3389/fmars.2018.00234, 2018.

949　D'Ortenzio, F., Iudicone, D., Montegut, C. de B., Testor, P., Antoine, D., Marullo, S., Santoleri,

950　　　R. and Madec, G.: Seasonal variability of the mixed layer depth in the Mediterranean Sea

951　　　as derived from in situ profiles, Geophysical Research Letters, 32(12),

952　　　https://doi.org/10.1029/2005GL022463, 2005.

953　Duce, R. A., Liss, P. S., Merrill, J. T., Atlas, E. L., Buat-Menard, P., Hicks, B. B., Miller, J. M.,

954　　　Prospero, J. M., Arimoto, R., Church, T. M., Ellis, W., Galloway, J. N., Hansen, L.,

955　　　Jickells, T. D., Knap, A. H., Reinhardt, K. H., Schneider, B., Soudine, A., Tokos, J. J.,

956　　　Tsunogai, S., Wollast, R. and Zhou, M.: The atmospheric input of trace species to the

957　　　world ocean, Global Biogeochemical Cycles, 5(3), 193–259,

958　　　https://doi.org/10.1029/91GB01778, 1991.

959　Dutkiewicz, S., Morris, J. J., Follows, M. J., Scott, J., Levitan, O., Dyhrman, S. T. and Berman-

960　　　Frank, I.: Impact of ocean acidification on the structure of future phytoplankton

961　　　communities, Nature Climate change, 5, 1002–1006, https://doi.org/10.1038/nclimate2722,

962　　　2015.

963   Emerson, S., Quay, P., Karl, D., Winn, C., Tupas, L. and Landry, M.: Experimental

964   determination of the organic carbon flux from open-ocean surface waters, Nature,

965   389(6654), 951–954, https://doi.org/10.1038/40111, 1997.

966   Falkovich, A. H., Ganor, E., Levin, Z., Formenti, P. and Rudich, Y.: Chemical and mineralogical

967   analysis of individual mineral dust particles, Journal of Geophysical Research:

968   Atmospheres, 106(D16), 18029–18036, https://doi.org/10.1029/2000JD900430, 2001.

969   Feliú, G., Pagano, M., Hidalgo, P. and Carlotti, F.: Structure and function of epipelagic

970   mesozooplankton and their response to dust deposition events during the spring

971   PEACETIME cruise in the Mediterranean Sea, Biogeosciences, 17, 5417–5441,

972   https://doi.org/10.5194/bg-17-5417-2020, 2020.

973   Gazeau, F., Van Wambeke, F., Marañón, E., Pérez-Lorenzo, M., Alliouane, S., Stolpe, C.,

974   Blasco, T., Leblond, N., Zäncker, B., Engel, A., Marie, B., Dinasquet, J. and Guieu, C.:

975   Impact of dust addition on the metabolism of Mediterranean plankton communities and

976   carbon export under present and future conditions of pH and temperature, Biogeosciences

977   Discussions, 2021.

978   Giovagnetti, V., Brunet, C., Conversano, F., Tramontano, F., Obernosterer, I., Ridame, C. and

979   Guieu, C.: Assessing the role of dust deposition on phytoplankton ecophysiology and

980   succession in a low-nutrient low-chlorophyll ecosystem: a mesocosm experiment in the

981   Mediterranean Sea, Biogeosciences, 10(5), 2973–2991, https://doi.org/10.5194/bg-10-

982   2973-2013, 2013.

983   Gorsky, G., Ohman, M. D., Picheral, M., Gasparini, S., Stemmann, L., Romagnan, J.-B.,

984   Cawood, A., Pesant, S., García-Comas, C. and Prejger, F.: Digital zooplankton image

985   analysis using the ZooScan integrated system, J Plankton Res, 32(3), 285–303,

986   https://doi.org/10.1093/plankt/fbp124, 2010.

987   Guieu, C. and Ridame, C.: Impact of atmospheric deposition on marine chemistry and

988   biogeochemistry, in Atmospheric Chemistry in the Mediterranean Region: Comprehensive

989   Diagnosis and Impacts, edited by F. Dulac, S. Sauvage, and E. Hamonou, Springer, Cham,

990   Switzerland, , 2020.

991   Guieu, C., Dulac, F., Desboeufs, K., Wagener, T., Pulido-Villena, E., Grisoni, J.-M., Louis, F.,

992   Ridame, C., Blain, S., Brunet, C., Bon Nguyen, E., Tran, S., Labiadh, M. and Dominici, J.-

993   M.: Large clean mesocosms and simulated dust deposition: a new methodology to

994   investigate responses of marine oligotrophic ecosystems to atmospheric inputs,

995   Biogeosciences, 7(9), 2765–2784, https://doi.org/10.5194/bg-7-2765-2010, 2010a.

996   Guieu, C., Loye-Pilot, M. D., Benyahya, L. and Dufour, A.: Spatial variability of atmospheric

997   fluxes of metals (Al, Fe, Cd, Zn and Pb) and phosphorus over the whole Mediterranean

998   from a one-year monitoring experiment: Biogeochemical implications, Marine Chemistry,

999   120(1–4), 164–178, https://doi.org/10.1016/j.marchem.2009.02.004, 2010b.

1000   Guieu, C., Ridame, C., Pulido-Villena, E., Bressac, M., Desboeufs, K. and Dulac, F.: Impact of

1001   dust deposition on carbon budget: a tentative assessment from a mesocosm approach,

1002   Biogeosciences, 11(19), 5621–5635, 2014a.

1003   Guieu, C., Aumont, O., Paytan, A., Bopp, L., Law, C. S., Mahowald, N., Achterberg, E. P.,

1004   Marañón, E., Salihoglu, B., Crise, A., Wagener, T., Herut, B., Desboeufs, K., Kanakidou,

1005   M., Olgun, N., Peters, F., Pulido-Villena, E., Tovar-Sanchez, A. and Völker, C.: The

1006   significance of the episodic nature of atmospheric deposition to Low Nutrient Low

1007   Chlorophyll regions, Global Biogeochemical Cycles, 28(11), 1179–1198,

1008   https://doi.org/10.1002/2014GB004852, 2014b.

1009   Guieu, C., D'Ortenzio, F., Dulac, F., Taillandier, V., Doglioli, A., Petrenko, A., Barrillon, S.,

1010   Mallet, M., Nabat, P. and Desboeufs, K.: Process studies at the air-sea interface after

1011   atmospheric deposition in the Mediterranean Sea: objectives and strategy of the

1012   PEACETIME oceanographic campaign (May–June 2017), Biogeosciences, 2020(17),

1013   5563–5585, https://doi.org/10.5194/bg-17-5563-2020, 2020.

Herut, B., Zohary, T., Krom, M. D., Mantoura, R. F. C., Pitta, P., Psarra, S., Rassoulzadegan, F., Tanaka, T. and Frede Thingstad, T.: Response of East Mediterranean surface water to Saharan dust: On-board microcosm experiment and field observations, Deep Sea Research Part II: Topical Studies in Oceanography, 52(22), 3024–3040, https://doi.org/10.1016/j.dsr2.2005.09.003, 2005.

Holmes, R. M., Aminot, A., Kérouel, R., Hooker, B. A. and Peterson, B. J.: A simple and precise method for measuring ammonium in marine and freshwater ecosystems, Can. J. Fish. Aquat. Sci., 56(10), 1801–1808, https://doi.org/10.1139/f99-128, 1999.

IPCC: Climate Change, The Physical Science Basis., 2013.

IPCC: IPCC Special Report on the Ocean and Cryosphere in a Changing Climate, edited by H. O. Pörtner, D. C. Roberts, V. Masson-Delmotte, P. Zhai, M. Tignor, E. Poloczanska, K. Mintenbeck, A. Alegría, M. Nicolai, A. Okem, J. Petzold, B. Rama, and N. M. Weyer., 2019.

Irwin, A. J. and Oliver, M. J.: Are ocean deserts getting larger?, Geophysical Research Letters, 36, https://doi.org/10.1029/2009gl039883, 2009.

Jickells, T. D., An, Z. S., Andersen, K. K., Baker, A. R., Bergametti, G., Brooks, N., Cao, J. J., Boyd, P. W., Duce, R. A., Hunter, K. A., Kawahata, H., Kubilay, N., laRoche, J., Liss, P. S., Mahowald, N., Prospero, J. M., Ridgwell, A. J., Tegen, I. and Torres, R.: Global Iron Connections Between Desert Dust, Ocean Biogeochemistry, and Climate, Science, 308(5718), 67–71, https://doi.org/10.1126/science.1105959, 2005.

Kana, T. M. and Glibert, P. M.: Effect of irradiances up to 2000 μE m^{-2} s^{-1} on marine *Synechococcus* WH7803—I. Growth, pigmentation, and cell composition, Deep Sea Research Part A. Oceanographic Research Papers, 34(4), 479–495, https://doi.org/10.1016/0198-0149(87)90001-X, 1987.

1038   Kapsenberg, L., Alliouane, S., Gazeau, F., Mousseau, L. and Gattuso, J.-P.: Coastal ocean

1039   acidification and increasing total alkalinity in the northwestern Mediterranean Sea, Ocean

1040   Science, 13, 411–426, https://doi.org/10.5194/os-13-411-2017, 2017.

1041   Kouvarakis, G., Mihalopoulos, N., Tselepides, A. and Stavrakakis, S.: On the importance of

1042   atmospheric inputs of inorganic nitrogen species on the productivity of the Eastern

1043   Mediterranean Sea, Global Biogeochemical Cycles, 15(4), 805–817,

1044   https://doi.org/10.1029/2001GB001399, 2001.

1045   Lagaria, A., Mandalakis, M., Mara, P., Papageorgiou, N., Pitta, P., Tsiola, A., Kagiorgi, M. and

1046   Psarra, S.: Phytoplankton response to Saharan dust depositions in the Eastern

1047   Mediterranean Sea: A mesocosm study, Front. Mar. Sci., 3,

1048   https://doi.org/10.3389/fmars.2016.00287, 2017.

1049   Law, C. S., Brévière, E., de Leeuw, G., Garçon, V., Guieu, C., Kieber, D. J., Kontradowitz, S.,

1050   Paulmier, A., Quinn, P. K., Saltzman, E. S., Stefels, J. and von Glasow, R.: Evolving

1051   research directions in Surface Ocean - Lower Atmosphere (SOLAS) science, Environ.

1052   Chem., 10(1), 1, https://doi.org/10.1071/EN12159, 2013.

1053   Lee, S. and Fuhrman, J. A.: Relationships between Biovolume and Biomass of Naturally Derived

1054   Marine Bacterioplankton, Appl Environ Microbiol, 53(6), 1298–1303, 1987.

1055   Lekunberri, I., Lefort, T., Romero, E., Vázquez-Domínguez, E., Romera-Castillo, C., Marrasé,

1056   C., Peters, F., Weinbauer, M. and Gasol, J. M.: Effects of a dust deposition event on

1057   coastal marine microbial abundance and activity, bacterial community structure and

1058   ecosystem function, J Plankton Res, 32(4), 381–396,

1059   https://doi.org/10.1093/plankt/fbp137, 2010.

1060   Liu, X., Patsavas, M. C. and Byrne, R. H.: Purification and Characterization of meta-Cresol

1061   Purple for Spectrophotometric Seawater pH Measurements, Environ. Sci. Technol., 45(11),

1062   4862–4868, https://doi.org/10.1021/es200665d, 2011.

1063   Longhurst, A., Sathyendranath, S., Platt, T. and Caverhill, C.: An estimate of global primary

1064   production in the ocean from satellite radiometer data, Journal of Plankton Research, 17(6),

1065   1245–1271, https://doi.org/10.1093/plankt/17.6.1245, 1995.

1066   López-Urrutia, A. and Morán, X. A. G.: Resource limitation of bacterial production distorts the

1067   temperature dependence of oceanic carbon cycling, Ecology, 88(4), 817–822,

1068   https://doi.org/10.1890/06-1641, 2007.

1069   Louis, J., Pedrotti, M. L., Gazeau, F. and Guieu, C.: Experimental evidence of formation of

1070   transparent exopolymer particles (TEP) and POC export provoked by dust addition under

1071   current and high pCO$_2$ conditions, PLOS ONE, 12(2), e0171980,

1072   https://doi.org/10.1371/journal.pone.0171980, 2017a.

1073   Louis, J., Guieu, C. and Gazeau, F.: Nutrient dynamics under different ocean acidification

1074   scenarios in a low nutrient low chlorophyll system: The Northwestern Mediterranean Sea,

1075   Estuarine, Coastal and Shelf Science, 186, 30–44,

1076   https://doi.org/10.1016/j.ecss.2016.01.015, 2017b.

1077   Louis, J., Gazeau, F. and Guieu, C.: Atmospheric nutrients in seawater under current and high

1078 pCO$_2$ conditions after Saharan dust deposition: Results from three minicosm experiments,

1079   Progress in Oceanography, 163, 40–49, https://doi.org/10.1016/j.pocean.2017.10.011,

1080   2018.

1081   Loÿe-Pilot, M. D. and Martin, J. M.: Saharan Dust Input to the Western Mediterranean: An

1082   Eleven Years Record in Corsica, in The Impact of Desert Dust Across the Mediterranean,

1083   edited by S. Guerzoni and R. Chester, pp. 191–199, Springer Netherlands, Dordrecht,

1084   https://doi.org/10.1007/978-94-017-3354-0_18, , 1996.

1085   Manca, B., Burca, M., Giorgetti, A., Coatanoan, C., Garcia, M.-J. and Iona, A.: Physical and

1086   biochemical averaged vertical profiles in the Mediterranean regions: an important tool to

1087   trace the climatology of water masses and to validate incoming data from operational

1088 oceanography, Journal of Marine Systems, 48(1), 83–116,

1089 https://doi.org/10.1016/j.jmarsys.2003.11.025, 2004.

1090 Marañón, E., Fernández, A., Mouriño-Carballido, B., MartÍnez-GarcÍa, S., Teira, E., Cermeño,

1091 P., Chouciño, P., Huete-Ortega, M., Fernández, E., Calvo-DÍaz, A., Morán, X. A. G.,

1092 Bode, A., Moreno-Ostos, E., Varela, M. M., Patey, M. D. and Achterberg, E. P.: Degree of

1093 oligotrophy controls the response of microbial plankton to Saharan dust, Limnology and

1094 Oceanography, 55(6), 2339–2352, https://doi.org/10.4319/lo.2010.55.6.2339, 2010.

1095 Marañón, E., Lorenzo, M. P., Cermeño, P. and Mouriño-Carballido, B.: Nutrient limitation

1096 suppresses the temperature dependence of phytoplankton metabolic rates, The ISME

1097 Journal, 12(7), 1836–1845, https://doi.org/10.1038/s41396-018-0105-1, 2018.

1098 Marie, D., Simon, N., Guillou, L., Partensky, F. and Vaulot, D.: Flow cytometry analysis of

1099 marine picoplankton, in living color: protocols in flow cytometry and cell sorting, edited

1100 by R. A. Diamond and S. DeMaggio, pp. 421–454, Springer, Berlin, , 2010.

1101 Markaki, Z., Oikonomou, K., Kocak, M., Kouvarakis, G., Chaniotaki, A., Kubilay, N. and

1102 Mihalopoulos, N.: Atmospheric deposition of inorganic phosphorus in the Levantine Basin,

1103 eastern Mediterranean: Spatial and temporal variability and its role in seawater

1104 productivity, Limnology and Oceanography, 48(4), 1557–1568,

1105 https://doi.org/10.4319/lo.2003.48.4.1557, 2003.

1106 Maugendre, L., Gattuso, J.-P., Louis, J., de Kluijver, A., Marro, S., Soetaert, K. and Gazeau, F.:

1107 Effect of ocean warming and acidification on a plankton community in the NW

1108 Mediterranean Sea, ICES Journal of Marine Science, 72(6), 1744–1755,

1109 https://doi.org/10.1093/icesjms/fsu161, 2015.

1110 Maugendre, L., Guieu, C., Gattuso, J.-P. and Gazeau, F.: Ocean acidification in the

1111 Mediterranean Sea: Pelagic mesocosm experiments. A synthesis, Estuarine, Coastal and

1112 Shelf Science, 186, 1–10, https://doi.org/10.1016/j.ecss.2017.01.006, 2017.

1113   Mayot, N., D'Ortenzio, F., Ribera d'Alcalà, M., Lavigne, H. and Claustre, H.: Interannual

1114   variability of the Mediterranean trophic regimes from ocean color satellites,

1115   Biogeosciences, 13(6), 1901–1917, https://doi.org/10.5194/bg-13-1901-2016, 2016.

1116   Mélançon, J., Levasseur, M., Lizotte, M., Scarratt, M., Tremblay, J.-É., Tortell, P., Yang, G.-P.,

1117   Shi, G.-Y., Gao, H., Semeniuk, D., Robert, M., Arychuk, M., Johnson, K., Sutherland, N.,

1118   Davelaar, M., Nemcek, N., Peña, A. and Richardson, W.: Impact of ocean acidification on

1119   phytoplankton assemblage, growth, and DMS production following Fe-dust additions in

1120   the NE Pacific high-nutrient, low-chlorophyll waters, Biogeosciences, 13(5), 1677–1692,

1121   https://doi.org/10.5194/bg-13-1677-2016, 2016.

1122   Moore, C. M., Mills, M. M., Arrigo, K. R., Berman-Frank, I., Bopp, L., Boyd, P. W., Galbraith,

1123   E. D., Geider, R. J., Guieu, C., Jaccard, S. L., Jickells, T. D., La Roche, J., Lenton, T. M.,

1124   Mahowald, N. M., Marañón, E., Marinov, I., Moore, J. K., Nakatsuka, T., Oschlies, A.,

1125   Saito, M. A., Thingstad, T. F., Tsuda, A. and Ulloa, O.: Processes and patterns of oceanic

1126   nutrient limitation, Nature Geoscience, 6(9), 701–710, https://doi.org/10.1038/ngeo1765,

1127   2013.

1128   Morán, X. A. G., López-Urrutia, Á., Calvo-Díaz, A. and Li, W. K. W.: Increasing importance of

1129   small phytoplankton in a warmer ocean, Global Change Biology, 16(3), 1137–1144,

1130   https://doi.org/10.1111/j.1365-2486.2009.01960.x, 2010.

1131   Neale, P. J., Sobrino, C., Segovia, M., Mercado, J. M., Leon, P., Cortés, M. D., Tuite, P., Picazo,

1132   A., Salles, S., Cabrerizo, M. J., Prasil, O., Montecino, V., Reul, A. and Fuentes-Lema, A.:

1133   Effect of CO_2, nutrients and light on coastal plankton. I. Abiotic conditions and biological

1134   responses, Aquatic Biology, 22, 25–41, https://doi.org/10.3354/ab00587, 2014.

1135   Obernosterer, I., Kawasaki, N. and Benner, R.: P-limitation of respiration in the Sargasso Sea

1136   and uncoupling of bacteria from P-regeneration in size-fractionation experiments, Aquatic

1137   Microbial Ecology, 32(3), 229–237, https://doi.org/10.3354/ame032229, 2003.

1138   Orr, J. C., Epitalon, J.-M., Dickson, A. G. and Gattuso, J.-P.: Routine uncertainty propagation for

1139   the marine carbon dioxide system, Marine Chemistry, 207, 84–107,

1140   https://doi.org/10.1016/j.marchem.2018.10.006, 2018.

1141   Paytan, A., Mackey, K. R. M., Chen, Y., Lima, I. D., Doney, S. C., Mahowald, N., Labiosa, R.

1142   and Post, A. F.: Toxicity of atmospheric aerosols on marine phytoplankton, Proceedings of

1143   the National Academy of Sciences, 106(12), 4601–4605,

1144   https://doi.org/10.1073/pnas.0811486106, 2009.

1145   Pitta, P., Kanakidou, M., Mihalopoulos, N., Christodoulaki, S., Dimitriou, P. D., Frangoulis, C.,

1146   Giannakourou, A., Kagiorgi, M., Lagaria, A., Nikolaou, P., Papageorgiou, N., Psarra, S.,

1147   Santi, I., Tsapakis, M., Tsiola, A., Violaki, K. and Petihakis, G.: Saharan Dust Deposition

1148   Effects on the Microbial Food Web in the Eastern Mediterranean: A Study Based on a

1149   Mesocosm Experiment, Front. Mar. Sci., 4, https://doi.org/10.3389/fmars.2017.00117,

1150   2017.

1151   Polovina, J. J., Howell, E. A. and Abecassis, M.: Ocean's least productive waters are expanding,

1152   Geophysical Research Letters, 35(3), https://doi.org/10.1029/2007gl031745, 2008.

1153   Powley, H. R., Krom, M. D. and Cappellen, P. V.: Understanding the unique biogeochemistry of

1154   the Mediterranean Sea: Insights from a coupled phosphorus and nitrogen model, Global

1155   Biogeochemical Cycles, 31(6), 1010–1031, https://doi.org/10.1002/2017GB005648, 2017.

1156   Pulido-Villena, E., Wagener, T. and Guieu, C.: Bacterial response to dust pulses in the western

1157   Mediterranean: Implications for carbon cycling in the oligotrophic ocean, Global

1158   Biogeochemical Cycles, 22(1), https://doi.org/10.1029/2007gb003091, 2008.

1159   Pulido-Villena, E., Rerolle, V. and Guieu, C.: Transient fertilizing effect of dust in P-deficient

1160   LNLC surface ocean, Geophysical Research Letters, 37,

1161   https://doi.org/10.1029/2009gl041415, 2010.

1162   Pulido-Villena, E., Baudoux, A.-C., Obernosterer, I., Landa, M., Caparros, J., Catala, P.,

1163   Georges, C., Harmand, J. and Guieu, C.: Microbial food web dynamics in response to a

1164   Saharan dust event: results from a mesocosm study in the oligotrophic Mediterranean Sea,

1165   Biogeosciences, 11(19), 5607–5619, 2014.

1166 Putaud, J.-P., Dingenen, R. V., Dell'Acqua, A., Raes, F., Matta, E., Decesari, S., Facchini, M. C.

1167   and Fuzzi, S.: Size-segregated aerosol mass closure and chemical composition in Monte

1168   Cimone (I) during MINATROC, Atmospheric Chemistry and Physics, 4(4), 889–902,

1169   https://doi.org/10.5194/acp-4-889-2004, 2004.

1170 Ras, J., Claustre, H. and Uitz, J.: Spatial variability of phytoplankton pigment distributions in the

1171   Subtropical South Pacific Ocean: comparison between in situ and predicted data,

1172   Biogeosciences, 5(2), 353–369, https://doi.org/10.5194/bg-5-353-2008, 2008.

1173 Regaudie-de-Gioux, A., Vaquer-Sunyer, R. and Duarte, C. M.: Patterns in planktonic

1174   metabolism in the Mediterranean Sea, Biogeosciences, 6(12), 3081–3089,

1175   https://doi.org/10.5194/bg-6-3081-2009, 2009.

1176 Richon, C., Dutay, J.-C., Dulac, F., Wang, R., Balkanski, Y., Nabat, P., Aumont, O., Desboeufs,

1177   K., Laurent, B., Guieu, C., Raimbault, P. and Beuvier, J.: Modeling the impacts of

1178   atmospheric deposition of nitrogen and desert dust-derived phosphorus on nutrients and

1179   biological budgets of the Mediterranean Sea, Progress in Oceanography, 163, 21–39,

1180   https://doi.org/10.1016/j.pocean.2017.04.009, 2018.

1181 Ridame, C. and Guieu, C.: Saharan input of phosphate to the oligotrophic water of the open

1182   western Mediterranean Sea, Limnology and Oceanography, 47(3), 856–869, 2002.

1183 Ridame, C., Guieu, C. and L'Helguen, S.: Strong stimulation of N 2 fixation in oligotrophic

1184   Mediterranean Sea: results from dust addition in large in situ mesocosms, Biogeosciences,

1185   10(11), 7333–7346, 2013.

1186 Ridame, C., Dekaezemacker, J., Guieu, C., Bonnet, S., L'Helguen, S. and Malien, F.: Contrasted

1187   Saharan dust events in LNLC environments: impact on nutrient dynamics and primary

1188   production, Biogeosciences (BG), 11(17), 4783–4800, 2014.

1189   Romero, E., Peters, F., Marrasé, C., Guadayol, Ò., Gasol, J. M. and Weinbauer, M. G.: Coastal

1190   Mediterranean plankton stimulation dynamics through a dust storm event: An experimental

1191   simulation, Estuarine, Coastal and Shelf Science, 93(1), 27–39,

1192   https://doi.org/10.1016/j.ecss.2011.03.019, 2011.

1193   Roy-Barman, M., Folio, L., Douville, E., Leblond, N., Gazeau, F., Bressac, M., Wagener, T.,

1194   Ridame, C., Desboeufs, K. and Guieu, C.: Contrasted release of insoluble elements (Fe, Al,

1195   REE, Th, Pa) after dust deposition in seawater: a tank experiment approach,

1196   Biogeosciences Discussions, 1–27, https://doi.org/10.5194/bg-2020-247, 2020.

1197   Sala, M. M., Aparicio, F. L., Balagué, V., Boras, J. A., Borrull, E., Cardelús, C., Cros, L.,

1198   Gomes, A., López-Sanz, A., Malits, A., Martínez, R. A., Mestre, M., Movilla, J., Sarmento,

1199   H., Vázquez-Domínguez, E., Vaqué, D., Pinhassi, J., Calbet, A., Calvo, E., Gasol, J. M.,

1200   Pelejero, C. and Marrasé, C.: Contrasting effects of ocean acidification on the microbial

1201   food web under different trophic conditions, ICES Journal of Marine Science, 73(3), 670–

1202   679, https://doi.org/10.1093/icesjms/fsv130, 2016.

1203   Sherr, E. B. and Sherr, B. F.: Bacterivory and herbivory: Key roles of phagotrophic protists in

1204   pelagic food webs, Microb Ecol, 28(2), 223–235, https://doi.org/10.1007/BF00166812,

1205   1994.

1206   Siokou-Frangou, I., Christaki, U., Mazzocchi, M. G., Montresor, M., Ribera d'Alcalá, M.,

1207   Vaqué, D. and Zingone, A.: Plankton in the open Mediterranean Sea: a review,

1208   Biogeosciences, 7(5), 1543–1586, https://doi.org/10.5194/bg-7-1543-2010, 2010.

1209   Tanaka, T., Thingstad, T. F., Christaki, U., Colombet, J., Cornet-Barthaux, V., Courties, C.,

1210   Grattepanche, J.-D., Lagaria, A., Nedoma, J., Oriol, L., Psarra, S., Pujo-Pay, M. and

1211   Wambeke, F. V.: Lack of P-limitation of phytoplankton and heterotrophic prokaryotes in

1212   surface waters of three anticyclonic eddies in the stratified Mediterranean Sea,

1213   Biogeosciences, 8(2), 525–538, https://doi.org/10.5194/bg-8-525-2011, 2011.

1214   Ternon, E., Guieu, C., Loÿe-Pilot, M.-D., Leblond, N., Bosc, E., Gasser, B., Miquel, J.-C. and

1215   Martín, J.: The impact of Saharan dust on the particulate export in the water column of the

1216   North Western Mediterranean Sea, Biogeosciences, 7(3), 809–826,

1217   https://doi.org/10.5194/bg-7-809-2010, 2010.

1218   The Mermex group: Marine ecosystems' responses to climatic and anthropogenic forcings in the

1219   Mediterranean, Progress in Oceanography, 91(2), 97–166,

1220   https://doi.org/10.1016/j.pocean.2011.02.003, 2011.

1221   Theodosi, C., Markaki, Z., Tselepides, A. and Mihalopoulos, N.: The significance of atmospheric

1222   inputs of soluble and particulate major and trace metals to the eastern Mediterranean

1223   seawater, Marine Chemistry, 120(1), 154–163,

1224   https://doi.org/10.1016/j.marchem.2010.02.003, 2010.

1225   Van Wambeke, F., Goutx, M., Striby, L., Sempéré, R. and Vidussi, F.: Bacterial dynamics

1226   during the transition from spring bloom to oligotrophy in the northwestern Mediterranean

1227   Sea: relationships with particulate detritus and dissolved organic matter, Marine Ecology

1228   Progress Series, 212, 89–105, 2001.

1229   Van Wambeke, F., Taillandier, V., Deboeufs, K., Pulido-Villena, E., Dinasquet, J., Engel, A.,

1230   Marañón, E., Ridame, C. and Guieu, C.: Influence of atmospheric deposition on

1231   biogeochemical cycles in an oligotrophic ocean system, Biogeosciences Discussions, 1–51,

1232   https://doi.org/10.5194/bg-2020-411, 2020a.

1233   Van Wambeke, F., Pulido, E., Dinasquet, J., Djaoudi, K., Engel, A., Garel, M., Guasco, S.,

1234   Nunige, S., Taillandier, V., Zäncker, B. and Tamburini, C.: Spatial patterns of biphasic

1235   ectoenzymatic kinetics related to biogeochemical properties in the Mediterranean Sea,

1236   Biogeosciences Discussions, 1–38, https://doi.org/10.5194/bg-2020-253, 2020b.

1237   Verity, P. G., Robertson, C. Y., Tronzo, C. R., Andrews, M. G., Nelson, J. R. and Sieracki, M.

1238   E.: Relationships between cell volume and the carbon and nitrogen content of marine

1239   photosynthetic nanoplankton, Limnology and Oceanography, 37(7), 1434–1446,

1240   https://doi.org/10.4319/lo.1992.37.7.1434, 1992.

1241 Vidussi, F., Claustre, H., Manca, B. B., Luchetta, A. and Marty, J.-C.: Phytoplankton pigment

1242   distribution in relation to upper thermocline circulation in the eastern Mediterranean Sea

1243   during winter, Journal of Geophysical Research: Oceans, 106(C9), 19939–19956,

1244   https://doi.org/10.1029/1999JC000308, 2001.

1245

1246 Table 1. List of parameters and processes investigated during the three experiments at stations

1247 TYR, ION and FAST. Related manuscripts are indicated. pH_T: pH on the total scale, A_T: total

1248 alkalinity, $^{13}C-C_T$: ^{13}C signature of dissolved inorganic carbon, NO_x: nitrate + nitrite, DIP:

1249 dissolved inorganic phosphorus, $Si(OH)_4$: silicate, DFe: dissolved iron, DAl: dissolved

1250 aluminium, Th-REE-Pa: Thorium (^{230}Th and ^{232}Th), Rare Earth elements and Protactinium

1251 (^{231}Pa), POC: particulate organic carbon, DOC: dissolved organic carbon, ^{13}C-DOC: ^{13}C

1252 signature of dissolved organic carbon, TEP: transparent exopolymer particles, NCP/CR: net

1253 community production and community respiration (oxygen based), ^{14}C-PP: primary production

1254 based on ^{14}C incorporation.

1255

1256

1257
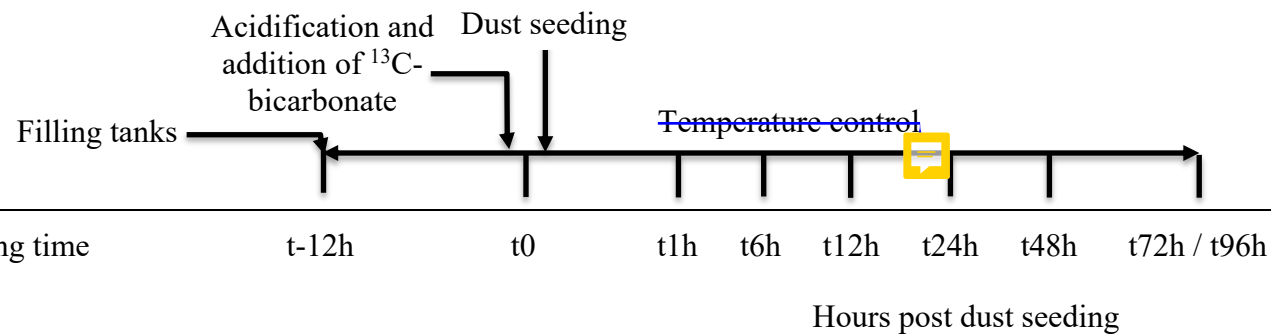
	Related manuscript
Temperature	This manuscript
Continuous	
Irradiance	This manuscript
Continuous	

Carbonate chemistry

pH$_T$ — This manuscript

A_T — This manuscript

δ^{13}C-C_T — Gazeau et al. (2021)

Macro-nutrients

NO$_x$ — This manuscript

DIP — This manuscript

Si(OH)$_4$ — This manuscript

Micro-nutrients

DFe — Roy-Barman et al. (2020)

DAl — Roy-Barman et al. (2020)

Th-REE-Pa — Roy-Barman et al. (2020)

Biological stocks

Pigments — This manuscript

Flow cytometry — This manuscript

Microscopy			This manuscript
Diazotroph abundance			Céline Ridame (unpublished)
Virus abundance			Dinasquet et al. (2021)
Meta-transcriptomics			Dinasquet et al. (2021)
Bacterial diversity			Dinasquet et al. (2021)
Micro-eukaryote diversity			Dinasquet et al. (2021)
Meso-zooplankton			This manuscript
POC (incl. δ^{13}C)			Gazeau et al. (2021)
POC sediment traps			Gazeau et al. (2021)
DOC			Gazeau et al. (2021)
^{13}C-DOC			Gazeau et al. (2021)
TEP			Gazeau et al. (2021)
Amino acids			Gazeau et al. (2021)
Carbohydrates			Gazeau et al. (2021)
Processes			

NCP/CR		Gazeau et al. (2021)
^{14}C-PP		Gazeau et al. (2021)
heterotrophic production		Gazeau et al. (2021)
Ectoenzymatic activity		Gazeau et al. (2021)
N$_2$ fixation		Céline Ridame (unpublished)
^{13}CO$_2$-fixation		Céline Ridame (unpublished), Gazeau et al. (2021?)
Virus production, lysogeny		Dinasquet et al. (2021)

1258

1259 Table 2. Initial conditions ~~as~~ measured while filling the tanks ~~(initial conditions in pumped~~

1260 ~~surface water; sampling time: t-12h).~~ pH$_T$: pH on the total scale, NO$_x$: nitrate + nitrite, NH$_4$:

1261 ammonium, DIP: dissolved inorganic phosphorus, Si(OH)$_4$: silicate, TChl$a$: total chlorophyll a,

1262 HNF: heterotrophic nanoflagellates. The three most important pigments in terms of concentration

1263 are also presented (19'-hexanoyloxyfucoxanthin, Zeaxanthin and Divinyl Chlorophyll a).

1264 Biomasses of the different groups analyzed through flow cytometry were estimated based on

1265 conversion equations and/or factors found in the literature (see section 2.3). Autotrophic biomass

1266 ~~was, as a first approximation, estimated only~~ based on flow cytometry ~~data and therefore~~

1267 ~~corresponds to the~~ fraction < 20 µm. ~~Heterotrophic biomass was estimated as the sum of~~

1268 ~~heterotrophic prokaryote and HNF biomasses (see section 2.3.2).~~ Values below detection limits

1269 are indicated as < dl.

	Sampling station	TYR	ION	FAST
	Coordinates (decimal)	39.34 N, 12.60 E	35.49 N, 19.78 E	37.95 N, 2.90 N
	Bottom depth (m)	3395	3054	2775
	Day and time of sampling (local time)	17/05/2017 17:00	25/05/2017 17:00	02/06/2017 21:00
	Temperature (°C)	20.6	21.2	21.5
	Salinity	37.96	39.02	37.07
Carbonate	pH$_T$	8.04	8.07	8.03

chemistry	Total alkalinity (μmol kg^{-1})	2529	2627	2443
Nutrients	NO$_x$ (nmol L^{-1})	14.0	18.0	59.0
	NH$_4^+$ (μmol L^{-1})	0.045	0.022	< dl
	DIP (nmol L^{-1})	17.1	6.5	12.9
	Si(OH)$_4$ (μmol L^{-1})	1.0	0.96	0.64
	NO$_x$/DIP (molar ratio)	0.8	2.5	4.6
Pigments	TChl$a$ (μg L^{-1})	0.063	0.066	0.072
	19'-hexanoyloxyfucoxanthin (μg L^{-1})	0.017	0.021	0.016
	Zeaxanthin (μg L^{-1})	0.009	0.006	0.036
	Divinyl Chlorophyll a (μg L^{-1})	~ 0	0	0.014
Flow cytometry	Pico-eukaryotes (abundance in cell mL^{-1}; biomass in μg C L^{-1})	347.8; 0.5	239.9; 0.4	701.0; 1.0
	Nano-eukaryotes (abundance in cell mL^{-1}; biomass in μg C L^{-1})	150.5; 3.9	188.8; 4.8	196.6; 5.0
	Synechococcus (abundance in cell mL^{-1}; biomass in μg C L^{-1})	4972; 1.2	3037; 0.8	6406; 1.6
	Autotrophic biomass (μg C L^{-1})	5.6	6.0	7.7
	Heterotrophic prokaryotes abundance (x 10^5 cell mL^{-1})	4.79	2.14	6.15
	HNF (abundance in cell mL^{-1})	110.1	53.6	126.2
	Heterotrophic biomass (μg C L^{-1})	9.9	4.5	12.7
Microscopy	Pennate diatoms (abundance in cell L^{-1})	140	520	880
	Centric diatoms (abundance in cell L^{-1})	200	380	580

Dinoflagellates (abundance in cell L^{-1})	2770	3000	3410
Autotrophic flagellates (abundance in cell L^{-1})	0	60	650
Ciliates (abundance in cell L^{-1})	270	380	770

1270

Table 3. Maximum input of nitrate + nitrite (NO_x) and dissolved inorganic phosphorus (DIP) released from Saharan dust in tanks D and G as observed from the ~~two~~ discrete samplings ~~performed over~~ the first 6 h after seeding. The estimated maximal percentage of dissolution is also presented (see section 2.3.1 for details on the calculations).

	NO_x				DIP			
	D1	D2	G1	G2	D1	D2	G1	G2
Maximum input	μmol L^{-1}				nmol L^{-1}			
TYR	11.0	11.1	11.1	11.0	24.6	20.4	24.6	23.9
ION	11.2	11.6	11.2	11.3	23.3	22.0	19.6	22.9
FAST	11.3	11.1	11.1	11.2	30.8	31.3	36.9	29.8
~~Percentage of~~ dissolution (%)								
TYR	95	96	95	94	12	10	12	11
ION	96	99	96	97	11	10	9	11
FAST	97	97	95	97	15	15	17	14

1   Table 4. Removal rate of nitrate + nitrite (NO_x) and dissolved inorganic phosphorus (DIP) in

2   tanks D and G during the three experiments (TYR, ION and FAST). For NO_x, ~~decreasing~~ rates

3   were estimated based on linear regressions between maximal concentrations (i.e. after dust

4   enrichment, at t1h or t6h) and final concentrations (t72 h for TYR and ION and t96h for FAST).

5   For DIP, ~~decreasing~~ rates were estimated based on linear regressions between maximal

6   concentrations (i.e. after dust enrichment at t1h or t6h) and concentrations ~~measured at sampling~~

7   ~~times~~ after ~~which a~~ stabilization was observed. This sampling time is shown in parentheses. All

8   rates are expressed in nmol L^{-1} h^{-1}.

	NO$_x$			DIP		
	TYR	ION	FAST	TYR	ION	FAST
D1	-6.5	-8.6	-14.3	-0.4 (t72h)	-0.5 (t48h)	-0.2 (t96h)
D2	-1.0	-8.6	-13.5	-0.3 (t72h)	-0.8 (t24h)	-0.2 (t96h)
G1	-6.7	-13.1	-21.6	-1.3 (t24h)	-0.8 (t24h)	-1.5 (t24h)
G2	-0.8	-1.6	-25.2	-1.3 (t24h)	-1.6 (t24h)	-1.1 (t24h)

9

10 Table 5. Maximum relative changes in tanks D and G as compared to controls (average between

11 C1 and C2), ~~expressed as a %, for~~ the ~~three~~ experiments (TYR, ION and FAST). The sampling

12 time at which these maximum relative changes were observed is shown in brackets. Tchl$a$ refers

13 to the concentration of total chlorophyll a and B_{micro} to the biomass proxy of micro-

14 phytoplankton (sum of Fucoxanthin and Peridinin, see Material and Methods) based on high

15 performance liquid chromatography (HPLC). HP and HNF refer to heterotrophic prokaryote and

16 heterotrophic nanoflagellate abundances, respectively, ~~as~~ measured by flow cytometry.

Experiment	Tank	HPLC		Flow cytometry				
		TChl$a$	B_{micro}	Pico-eukaryotes	Nano-eukaryotes	*Synechococcus*	HP	HNF
TYR	D1	-35 (t24h)	-33 (t12h)	-75 (t72h)	-80 (t1h)	-71 (t48h)	68 (t72h)	352 (t72h)
TYR	D2	-38 (t12h)	-39 (t24h)	-75 (t72h)	-80 (t1h)	-72 (t48h)	53 (t72h)	100 (t72h)
TYR	G1	60 (t72h)	52 (t72h)	-75 (t1h)	89 (t72h)	76 (t72h)	67 (t72h)	1095 (t72h)
TYR	G2	359 (t72h)	392 (t72h)	323 (t72h)	119 (t72h)	700 (t72h)	68 (t48h)	298 (t72h)
ION	D1	183 (t72h)	157 (t72h)	126 (t72h)	89 (t72h)	317 (t72h)	128 (t72h)	44 (t72h)
ION	D2	109 (t72h)	156 (t72h)	117 (t72h)	-59 (t1h)	390 (t72h)	133 (t72h)	27 (t72h)
ION	G1	399 (t72h)	454 (t72h)	458 (t72h)	256 (t72h)	805 (t72h)	176 (t72h)	175 (t72h)

ION	G2	426 (t72h)	612 (t72h)	510 (t72h)	292 (t72h)	1425 (t72h)	161 (t72h)	129 (t72h)
FAST	D1	318 (t96h)	356 (t96h)	113 (t96h)	208 (t72h)	348 (t96h)	27 (t96h)	-38 (t96h)
FAST	D2	237 (t96h)	322 (t96h)	91 (t96h)	219 (t72h)	197 (t96h)	40 (t48h)	-49 (t96h)
FAST	G1	399 (t96h)	415 (t96h)	198 (t72h)	274 (t72h)	357 (t48h)	61 (t48h)	243 (t24h)
FAST	G2	395 (t96h)	421 (t96h)	129 (t72h)	202 (t96h)	344 (t48h)	67 (t48h)	74 (t24h)

17

Figure captions

Fig. 1. Location of the sampling stations in the Mediterranean Sea onboard the R/V "Pourquoi Pas ?" during the PEACETIME cruise, satellite-derived surface chlorophyll a concentration averaged over the entire duration of the cruise (Courtesy of Louise Rousselet).

Fig. 2. of an experimental tank (climate reactor).

Fig. 3. Proportion of the different pigments, as measured by high performance liquid chromatography (HPLC) in pumped surface seawater for the three experiments (t-12h).

Fig. 4. Continuous measurements of temperature and irradiance level (PAR) in the six tanks during the experiments. The dashed vertical line indicates the time of dust seeding (after t0).

Fig. 5. pH on the total scale (pH_T) and total alkalinity (A_T) measured in the six tanks during the experiments. The dashed vertical line indicates the time of dust seeding (after t0). Error bars correspond to the standard deviation based on analytical triplicates.

Fig. 6. Nutrients (nitrate + nitrite: NO_x, dissolved inorganic phosphorus: DIP, silicate: $Si(OH)_4$ molar ratio between NO_x and DIP, measured in tanks. The dashed vertical line indicates the time of seeding (after t0).

Fig. 7. total chlorophyll a and major pigments, high performance liquid chromatography (HPLC), in tanks The dashed vertical line indicates the time of seeding (after t0).

Fig. 8. Abundance of autotrophic pico-eukaryotes, autotrophic nano-eukaryotes, *Synechococcus,* heterotrophic prokaryotes (HP), and heterotrophic nano-flagellates (HNF), measured by flow cytometry, in the tanks during the experiments. The evolution of autotrophic biomass

(see Material and Methods for details on the calculation) is also shown. The dashed vertical line indicates the time of seeding (after t0).

Fig. 9. Abundances of meso-zooplankton species as measured at the end of each experiment.

Fig. 10. Maximal relative change (%) of main biological stocks (TCHla: total chlorophyll a, HP: heterotrophic prokaryotes) and processes (BP: bacterial production; PP: ^{14}C-based primary production; see Gazeau et al., 2021; BR: bacterial respiration (no data from this study); and N$_2$ fixation, Céline Ridame, unpublished results) as obtained during the present study at the 3 stations (TYR, ION and FAST) under ambient conditions of pH and temperature (open red squares) and future conditions (full green squares). Squares are delimited by the range of responses observed among the duplicates for each treatment. The dotted green squares for station TYR denote the large variability observed between duplicates for some parameters and processes that prevented drawing solid conclusions. Box-plots represent the distribution of responses observed from studies conducted in the Mediterranean Sea, as compiled by Guieu and Ridame (2020).
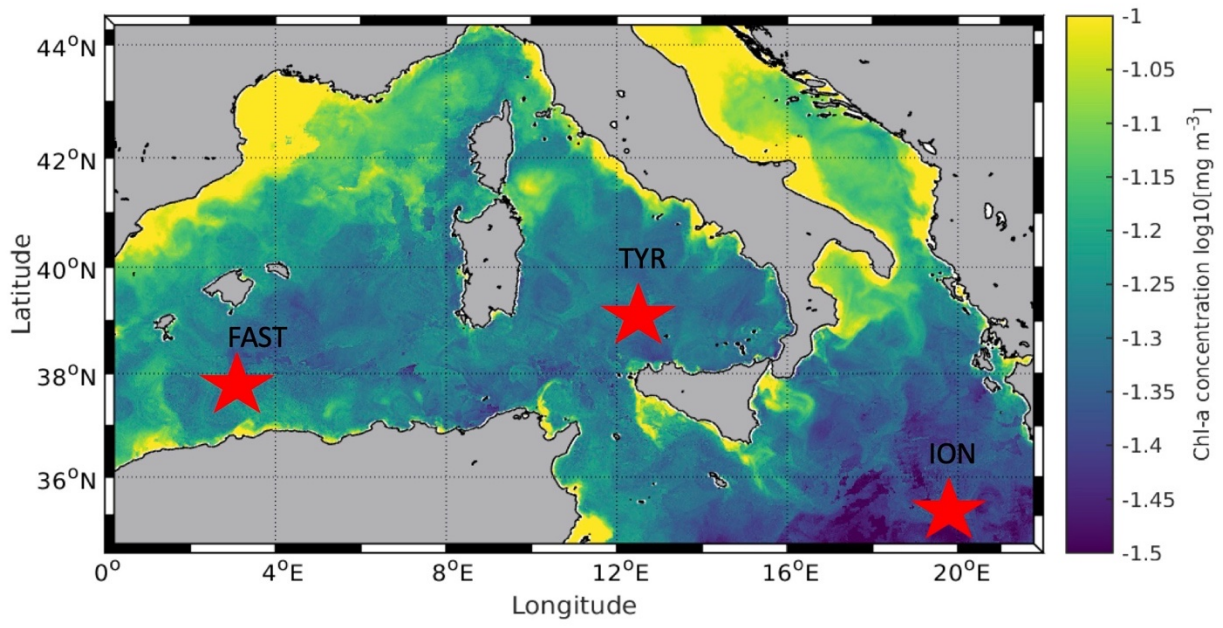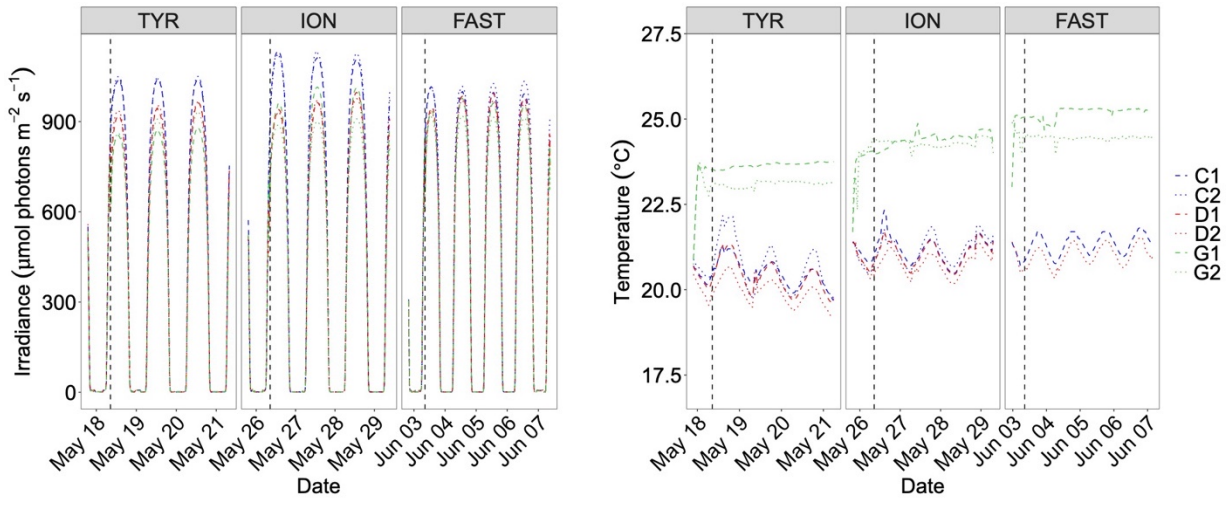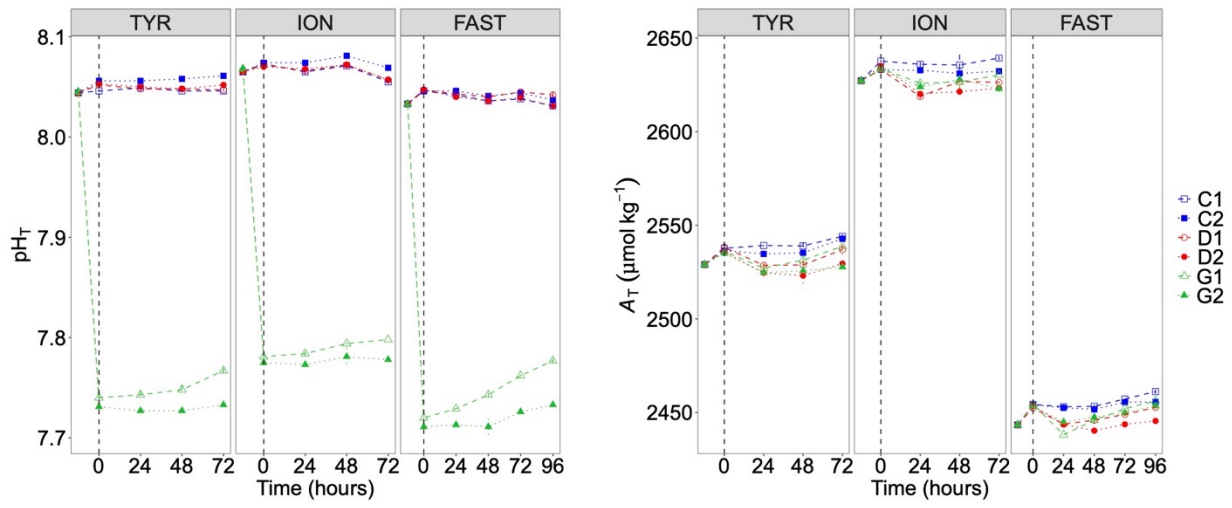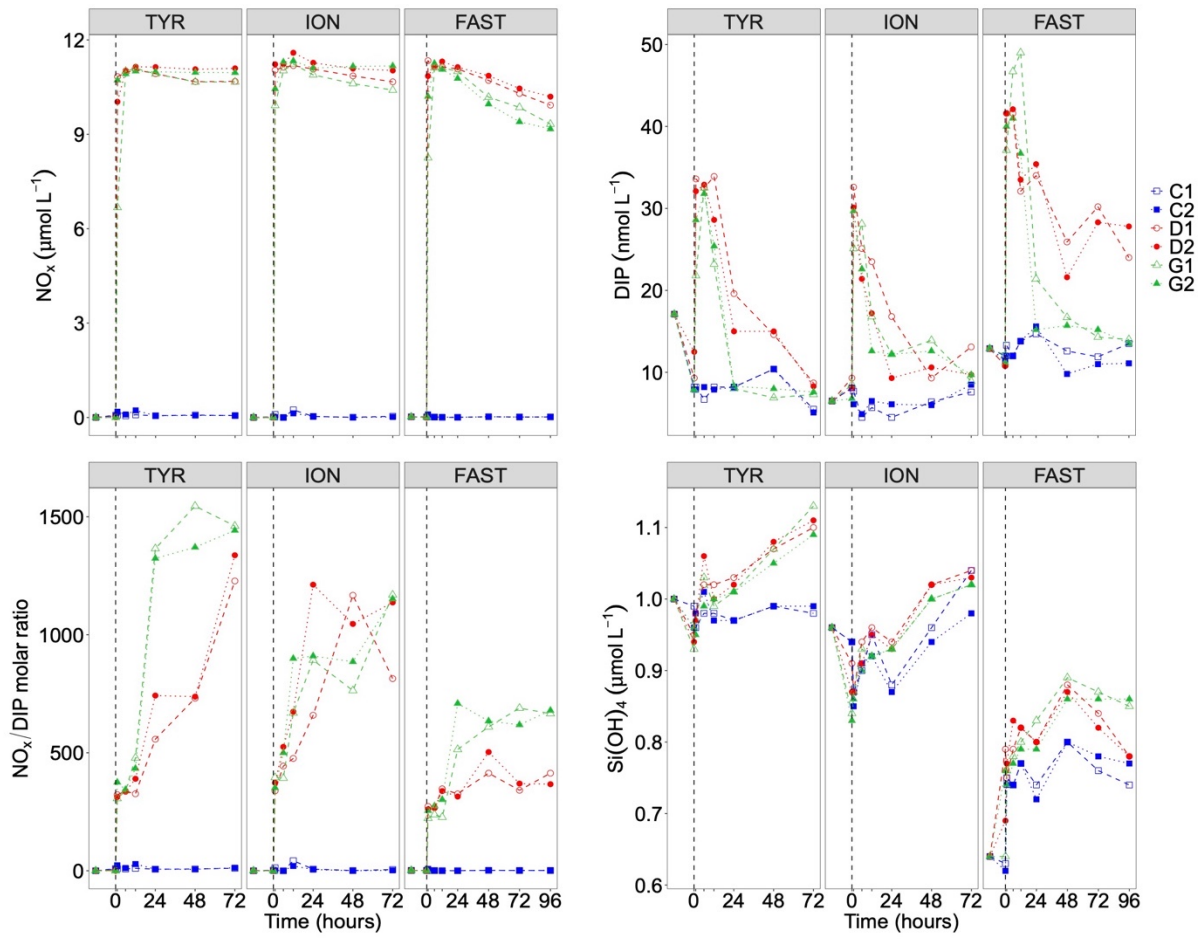
Fig. 1.
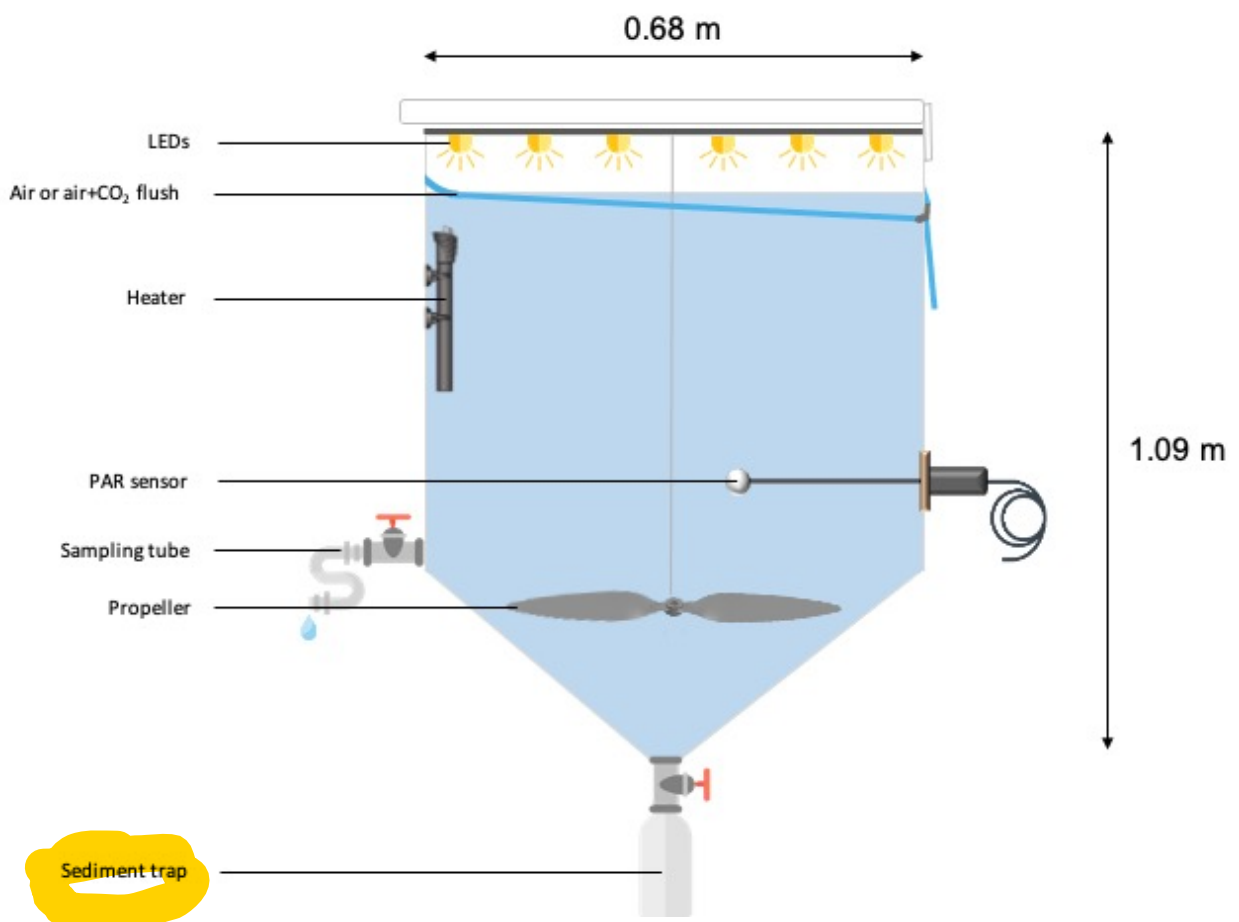
Fig. 2.
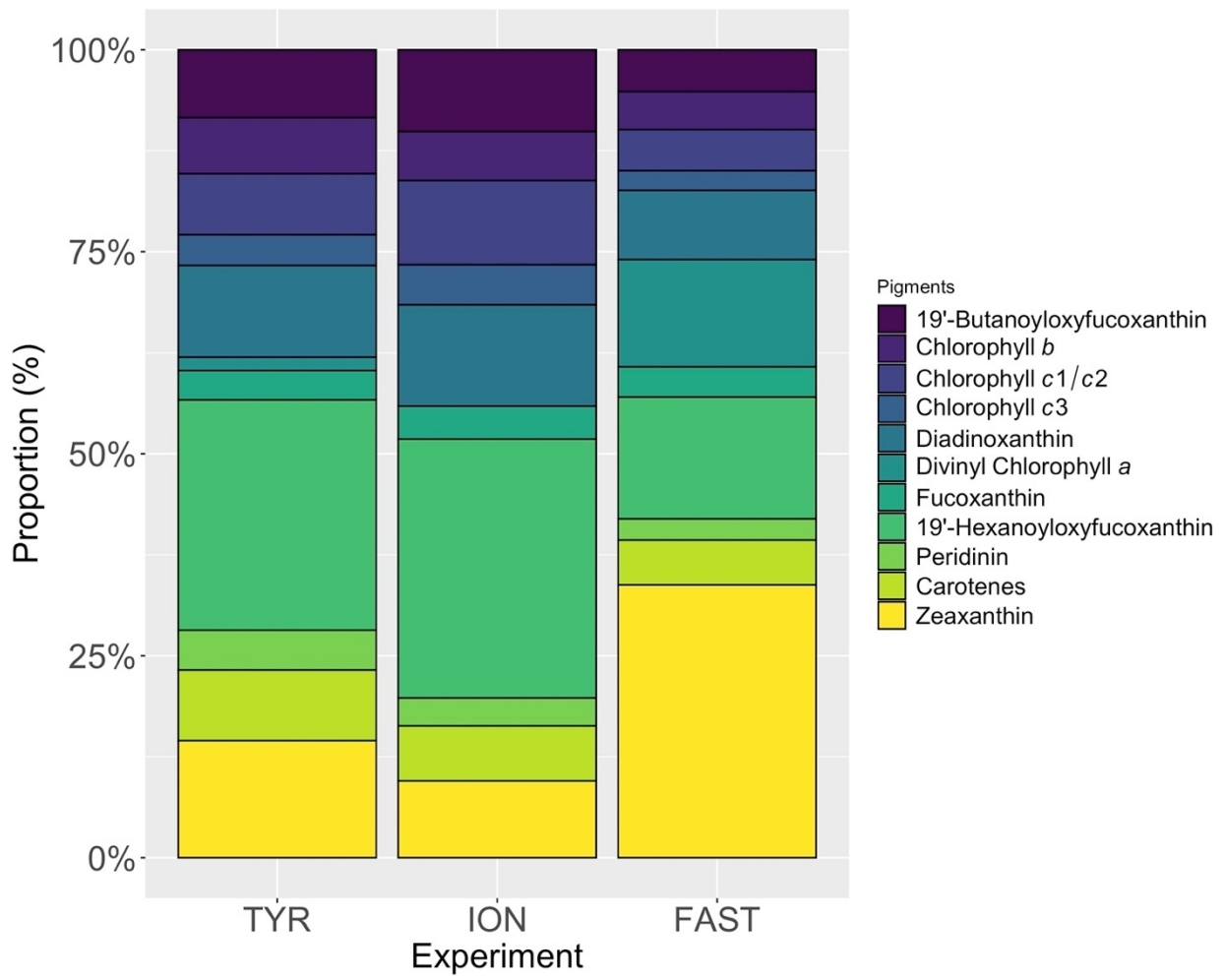
Fig. 3.

Fig. 4.

Fig. 5.

Fig. 6.

Fig. 7.
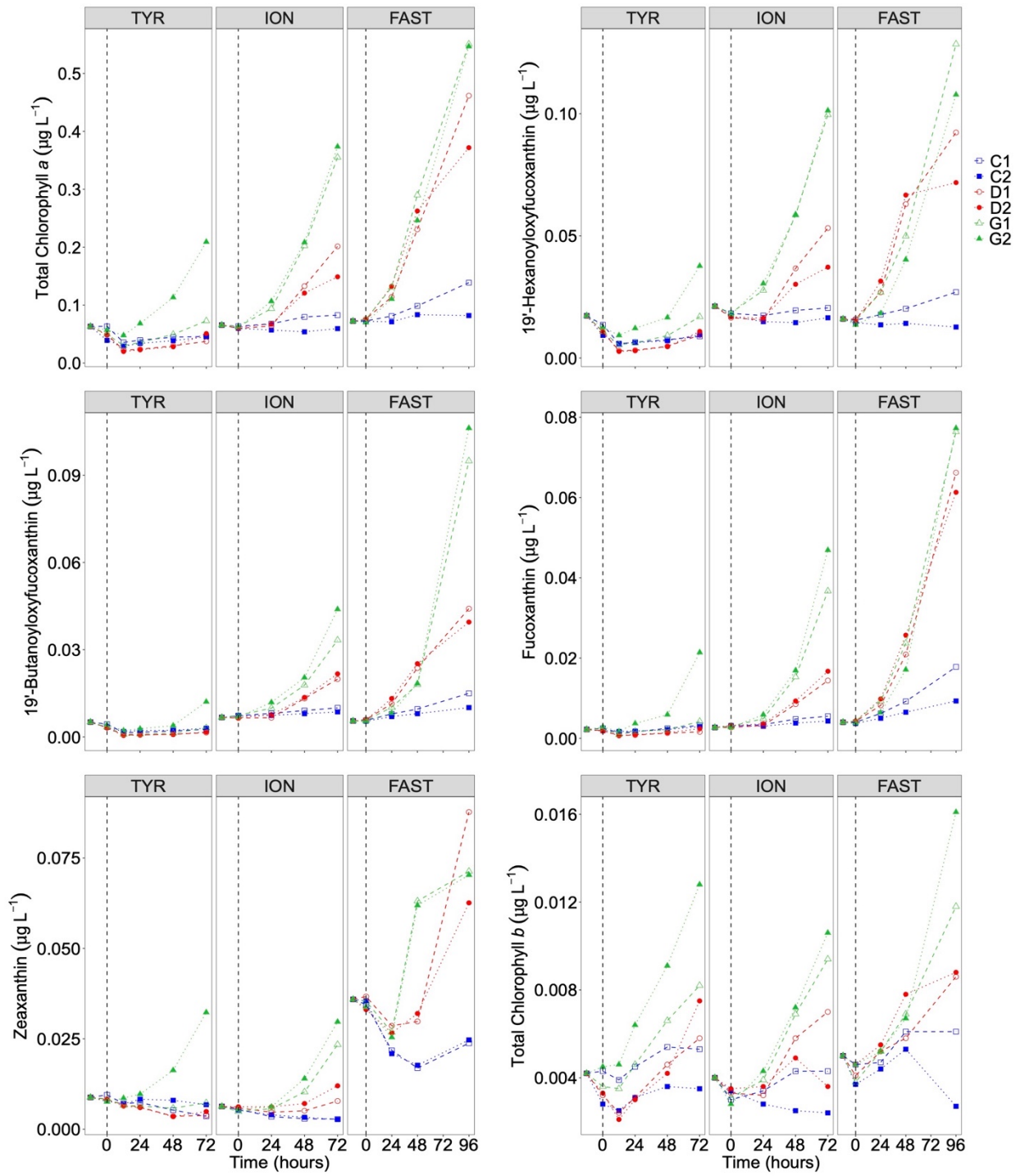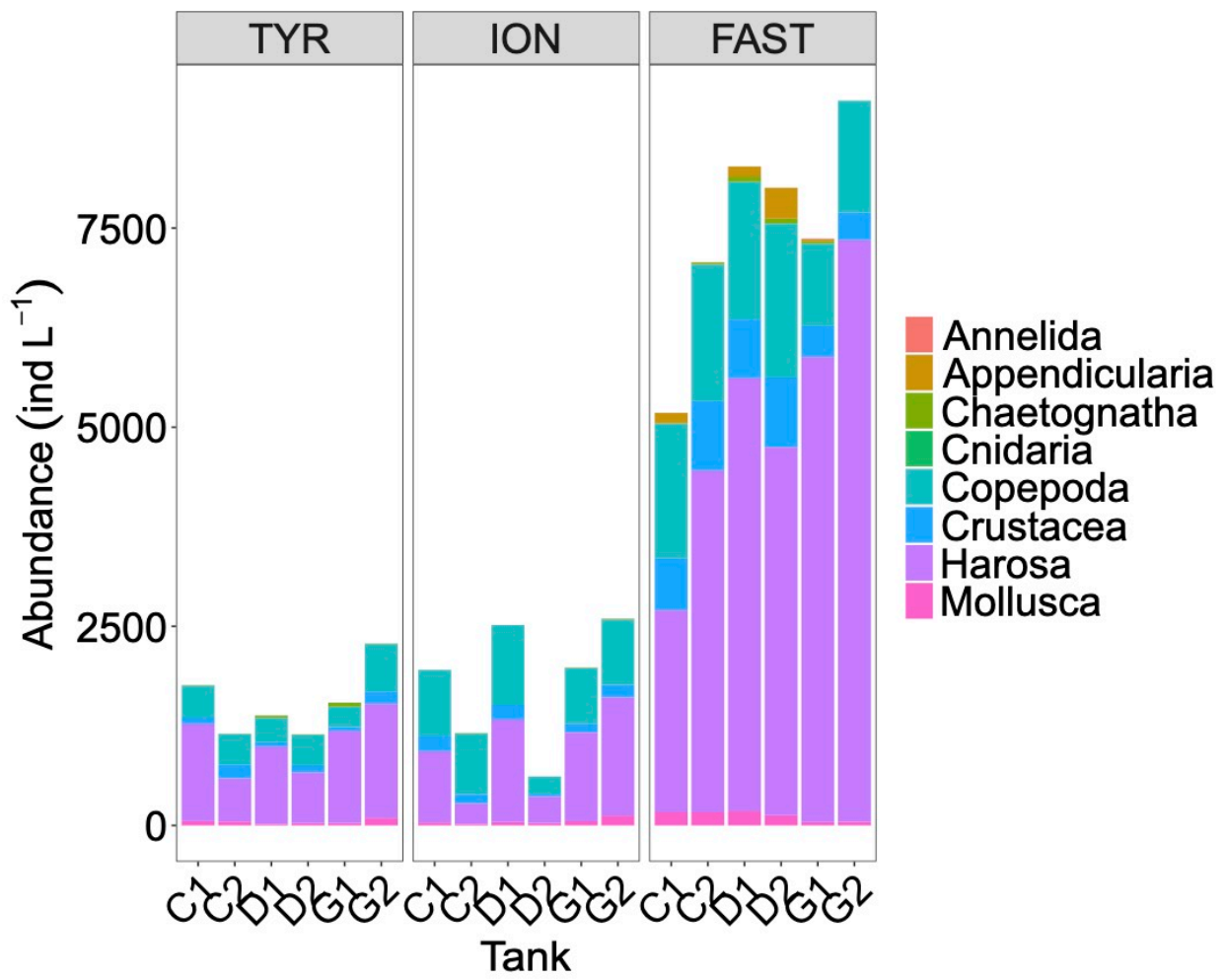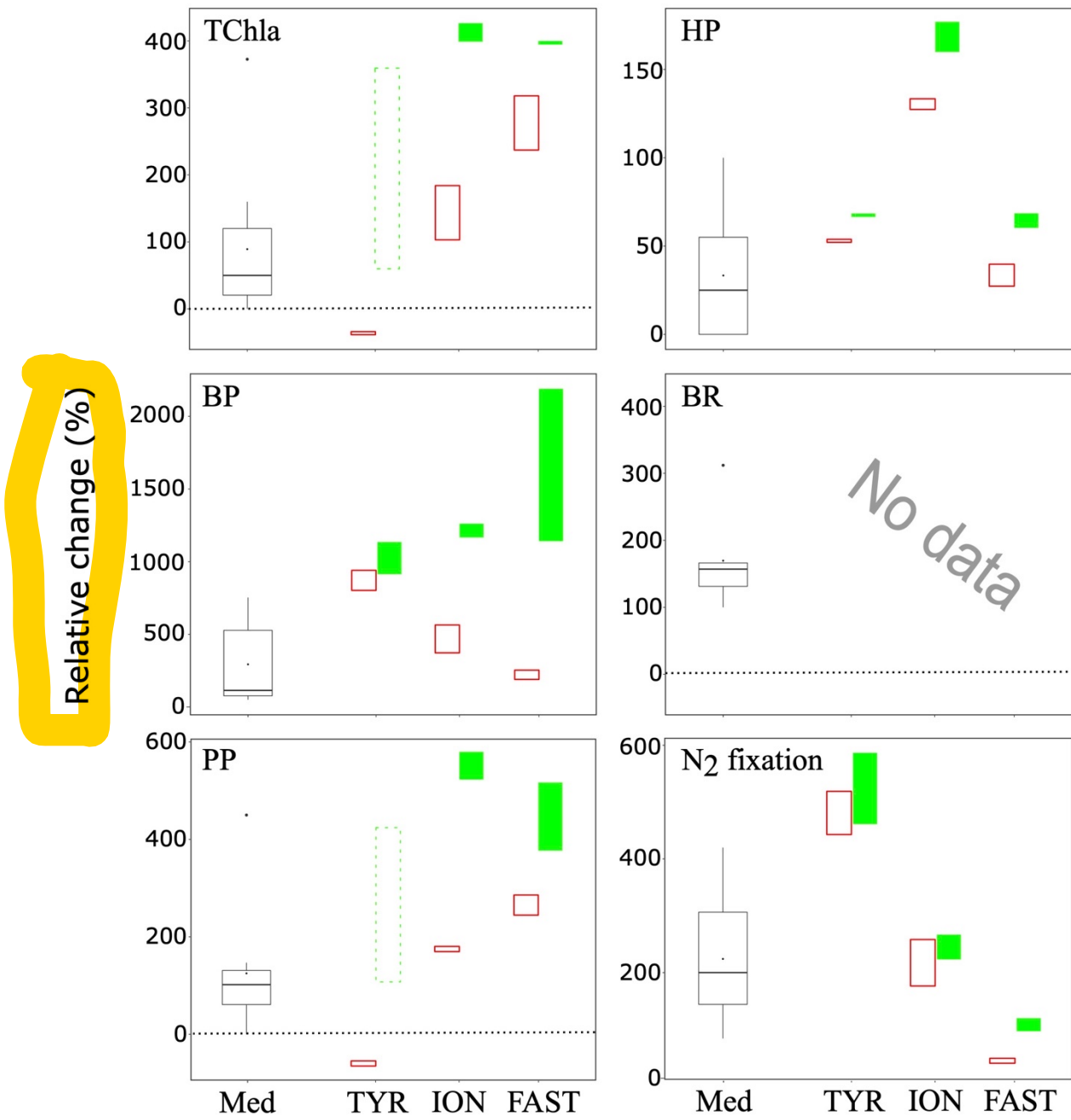
Fig. 8.

Fig. 9.

Relative change (%)

TChla · HP · BP · BR · No data · PP · N₂ fixation

Med   TYR   ION   FAST

Fig. 10.